Biosorption characteristics of methylene blue and malachite green from simulated wastewater onto *Carica papaya* wood biosorbent

Rangabhashiyam S*, Sujata Lata, Balasubramanian P*

Department of Biotechnology and Medical Engineering, National Institute of Technology Rourkela, Odisha-769 008, India

ABSTRACT

The present study reports the sequestration of the cationic dyes, methylene blue (MB) and malachite green (MG) from aqueous solutions using natural *Carica papaya* wood (CPW) in a batch biosorption process. Characterizations of CPW were achieved by Field Emission Scanning Electron Microscopy, X-ray Diffractometer and Fourier transform infrared spectroscopy. The influence of various parameters such as solution pH, biosorbent dose, contact time, initial dye concentration and temperature were examined and optimal experimental conditions were determined. The biosorption isotherm models and kinetics characteristic of dye biosorption onto CPW were investigated. The equilibrium data followed the Langmuir isotherm model, predicted the maximum biosorption capacities of 32.25 and 52.63 mg dye per gram of CPW for MB and MG, respectively. The biosorption kinetics of MB and MG removal using CPW was better described by the pseudo-second-order kinetic equation. The experimental data obtained at different temperature of 303, 313 and 323 K for the biosorption of each dyestuff using CPW were analyzed through the thermodynamic parameters of $\Delta G°$, $\Delta H°$ and $\Delta S°$ respectively. Experiments on the regeneration studies indicated that the biosorption capacity of CPW was consistent towards MB and MG removal upto 5 recycles by subjecting 0.1 M HCl as the desorbing agent. The current investigation revealed that the simulated wastewater showed better removal of MB and MG under the studied experimental conditions. Hence, the biomass from *Carica papaya* wood could be employed as an efficient, eco-friendly and economical biosorbent for the removal of MB and MG from industrial wastewater.

1. Introduction

Various classes of dyes finds their applications in the industrial sectors of textiles, rubber, paper and pulp, printing, paint, cosmetics, coke, petroleum, pesticide, leather, pharmaceutics, food and wood preservation [1]. More than 100,000 commercial dyes were produced worldwide and annual production was approximately 7×10^5–1×10^6 tons [2,3]. A significant amount of 10% dyes are lost during the industrial process, which consequently generates large quantities of dye containing wastewater and discharged into the local water bodies [4]. Dyes are colored organic compounds mostly belongs to synthetic origin. The complex aromatic structures make the synthetic dye resistant to the process of aerobic, anaerobic digestions, stable to light, heat, moderate oxidizing agents and difficult to biodegradation [5,6]. The significant colors of dyes deteriorate not only the aesthetic water properties, in addition raises the level of chemical oxygen demand (COD) biological oxygen demand (BOD), total suspended solids (TSS) and total dissolved solids (TDS), respectively [7]. The elevation of organic load by the dye substances in the water bodies inhibit the sunlight penetration resultant

in reduced photosynthetic activity of the autotrophic organisms and consequent to the ecological imbalance of the aquatic environment. Most of the synthetic dyes displays mutagenic, carcinogenic activity, causes hazardous health effects of kidney dysfunction, damage the central nervous system and reproductive system [8,9].

Methylene Blue (MB) is a common cationic dye, with its property of high adsorption ability generally utilized in the industrial process of dying cotton, silk and wool. MB also used as medicine in the treatment of some disease conditions of West Nile virus, Duck hepatitis B and psoriasis. The toxic effects of MB includes permanent injury to the eyes, breathing difficulties, gastritis, nausea, vomiting, mental confusion, tissue necrosis, painful micturition, cyanosis and methemoglobinemia like syndromes [10,11]. Malachite green (MG) is a cationic triphenylmethane dye used in the industries of silk, wool, leather, and distilleries. Medical applications of MG include the treatment against the infections of parasites, bacteria, fungi and as antiseptic in the industrial sector of aquaculture to control fish parasite and associated diseases [12]. The detrimental effects associated with MG are cytotoxic, carcinogenic, damage liver, intestine, gill, kidney, gonads and pituitary

Nomenclature

q_e	Amount of dye biosorbed at equilibrium (mg/g)
C_0	Initial concentration of the dye (mg/L)
C_e	Equilibrium concentration of dye (mg/L)
V	Volume of the dye solution (L)
m	Mass of the biosorbent (g)
pH_{PZC}	pH Zero Point Charge
R^2	Coefficient of determination
Q_0	Biosorption capacity from Langmuir isotherm (mg/g)
K_L	Langmuir isotherm constant (L/mg)
R_L	Langmuir isotherm model separation factor
K_F	Freundlich isotherm biosorption capacity (L/g)
n_F	Freundlich isotherm model coefficient
Q_m	Dubinin-Radushkevich isotherm maximum biosorption capacity (mg/g)
K	Dubinin-Radushkevich isotherm activity coefficient (mol^2/J^2)
ε	Polanyi potential of Dubinin–Radushkevich isotherm
R	Universal gas constant (8.314 J/mol K)
T	Temperature (K)
E	Mean biosorption energy (kJ/mol)
b_T	Temkin constant (kJ/mol)
A_T	Temkin isotherm equilibrium binding constant (L/g)
q_{mj}	Maximum biosorption capacity from Jovanovic isotherm (mg/g)
K_j	Jovanovic isotherm constant (L/g)
K_H	Halsey isotherm model constant
n_H	Halsey isotherm model exponent
Q	Degree of surface coverage
K_{FH}	Flory–Huggins isotherm model equilibrium constant
n_{FH}	Flory–Huggins isotherm model exponent
$k1$	Pseudo-first-order kinetic model rate constant (1/min)
k_2	Pseudo-second-order biosorption rate constant (g/mg min)
α	Initial rate of biosorption (mg/g min)
β	Elovich constant (g/mg)
k_{id}	Intraparticle diffusion model constant (mg/g $min^{0.5}$)
C	Boundary layer thickness (mg/g)
$\Delta G°$	Gibbs free energy change (kJ/mol)
$\Delta H°$	Enthalpy change (kJ/mol)
$\Delta S°$	Entropy change (J/mol K)
K_d	Distribution coefficient for biosorption

gonadotrophic cells, causes irritation to respiratory and gastrointestinal tract, skin redness and permanent eye injury [13]. The discharge of even low dye concentrations from the industrial effluents to the environment posed a significant threat due to their toxicological and aesthetic properties. To minimize the harmful effects associated with the dye contaminated wastewater to ecological environment and human health, proper treatment methods are obligatory before discharge into the water bodies [14,15]. The physical, chemical and biological methods such as sedimentation, anaerobic/aerobic treatment, coagulation/flocculation, electrokinetic coagulation, membrane technology, sonochemical degradation, ozonation, photochemical degradation, irradiation electrochemical degradation, biosorption and adsorption on activated carbon was generally employed for the removal of dye. On the basis of initial cost, simpler design and operation, insensitivity to toxic substances and minimal sludge generation, biosorption has been shown to be an effective method in the removal of toxic dye from aqueous solutions [16–19]. Biosorption of toxic dye on the lignocellulosic biomass has been identified as an appropriate alternative method, since the biosorbent utilization from the source of lignocellulosic materials are either natural material or agricultural wastes/byproducts are potential, cheap and environmental friendly. In comparison of all the methods, biosorption substantially reduces the costs connected with capital investment, operational and total treatment [20–22].

Wood biomass belongs to the lignocellulosic wastes, widely distributed, renewable and requires minimal further processing for biosorbent preparation. The biodegradability nature of the wood biosorbent offers further use as fertilizer [23]. Biomass is a complex material composed of polymeric materials like cellulose, lignin and other phenolic compounds. Biosorption process occurs through the affinity between polar functional groups of lignin in biosorbent and dye molecules [24]. Biosorbents such as hazelnut shell [25], coconut coir dust [26], lotus leaf [27], *Luffa cylindrica* fiber [28], Olive stone [29], *Lemna major* [30], Neem bark dust [31], spent rice biomass [32], tea waste [33], *Mansonia altissima* wood sawdust [34], yellow passion fruit waste [35], *Elaeagnus angustifolia* [36], *Ricinus communis* [37], rambutan peel [38], beech sawdust [39], Alligator Weed [40], Plantago ovata seeds [41], *Borassus aethiopum* flower [42], *Prosopis Cineraria* sawdust [43], maize husk leaf [44], degreased coffee bean [45], *Ricinus communis* presscake [46], were reported in the literatures on the biosorption of basic dyes from aqueous solution. Still there exists continuous research on

exploring efficient biosorbent for the removal of dyes from aqueous solutions. Carica papaya, commonly called as papaya is a large tree like herbaceous fruiting plant belongs to the family of Caricaceae. Carica papaya is native to the tropics of the America and the cultivation started first in South Mexico and Costa Rica. India is the leading papaya cultivator, followed with Brazil, Indonesia, Nigeria, Mexico, China, Thailand, Peru and Philippines [47]. The most important chemical constituents and percentage composition of the Carica papaya wood includes protein (4.96 ± 0.68%), crude fiber (30.11 ± 2.67%) and mineral ash (5.92 ± 1.02%). The crude fiber mainly composed of lignin and cellulose, representing the occurrence of hemicellulose and attached polysaccharides at higher level [48].

To our knowledge, the use of Carica papaya wood biomass as a biosorbent for the sequestration of MB and MG from aqueous solutions has not been investigated. The current research focuses on the dyes removal properties of Carica papaya wood (CPW), which is generated as a waste biomass and has no significant commercial value. Biosorption process variables of solution pH, biosorbent dose, initial dye concentration, contact time and temperature were optimized for the maximum dye biosorption. The dyes biosorption characteristics of CPW were correlated with the biosorption capacities, interaction mechanisms using biosorption isotherms and kinetic modeling. The thermodynamic parameters of the dyes biosorption process were also explored. The desorption efficiency of the dye loaded CPW was analyzed using 0.1 M HCl, in order to regenerate and reuse the CPW upto five cycles.

2. Materials and methods

2.1. Preparation of biosorbent

Biosorbent used in this work was wood biomass from *Carica papaya* (CPW), a common plant species cultivated in India. Papaya wood biomass was obtained from the fallen matured trunk. The barks of the obtained biomass was removed, cut into small pieces and washed thoroughly with distilled water in order to remove any adhering dirt. The washed wood pieces were oven dried at 110 °C for 24 h. The dried biomass was crushed and 100–200 µm fraction was selected as the size range of the biosorbent. The prepared biosorbent CPW was stored in an airtight plastic container in order to avoid moisture. CPW for the dye biosorption experiments was subjected in the natural form without any

additional pre-treatment.

2.2. Solutions and reagents

The basic dyes of Methylene Blue (MB) and Malachite Green (MG) are the model molecules used in the present study of biosorption without further purification. All the chemical reagents were of analytical grades. The stock solution of 1000 mg/L of MB and MG was prepared separately by dissolving accurately weighed amounts of each dye in 1000 mL distilled water. The required concentrations ranged between 10 and 50 mg/L of MB and MG were prepared by diluting the stock solution. Table 1 represents the molecular structure and general characteristics of MB and MG.

2.3. Determination of pH zero point charge (pH_{PZC})

The zero point charge of CPW was determined through the solid addition method, represents the pH at which the biosorbent surface has net electrically neutral [49]. 50 ml of potassium nitrate (0.1 M) was transferred to a series of 250 mL stoppered conical flasks. The initial pH of solutions was adjusted to the values of 2.0, 3.0, 4.0, 5.0, 6.0, 7.0, 8.0, 9.0 and 10.0 using either 0.1 M HCl or 0.1 M NaOH solution. Followed with that, 0.1 g of CPW was added to each flask and shaken for 24 h with agitation speed of 120 rpm at the temperature of 30 °C. Then the final solution pH (pH_f) was measured. The difference between the values of initial solution pH (pH_0) and final solution pH, (ΔpH = pH_0 − pH_f) were plotted against pH_0. The zero point charge of the CPW was found from the intersection point of the resulting curve at which ΔpH is zero.

2.4. Instrument analysis

The Fourier transform infrared spectroscopy (FT-IR) analysis of CPW was done using Perkin Elmer Spectrum Two in the range of 400–4000 cm^{-1}. The pattern of the X-ray diffraction (XRD) of CPW was recorded using Rigaku Ultima-IV. Field Emission Scanning Electron Microscopy (FE-SEM) Quanta 250 FEG was used to obtain the morphology of CPW.

2.5. Biosorption experimental procedure

The biosorption studies for assessment of the CPW for the removal of MB and MG dye from aqueous solutions was conducted by means of the batch biosorption procedure. The biosorption experiments was performed with initial pH of the dyes solution (2.0–10.0), fixed biosorbent dosage (0.02–0.18 g) using 50 mL of initial dye concentration (10.0–50.0 mg/L) placed in a 250 mL stoppered conical flasks and agitated in a thermostated shaking incubator at 120 rpm for a suitable contact time (10.0–140.0 min) at the different temperature range (303–333 K). At a pre-determined time intervals, the samples were withdrawn for residual analysis of MB and MG concentrations determined using a double beam UV–visible spectrophotometer (Systronics 2203).

The amount of dye biosorbed onto per gram of CPW was calculated according the following equation

$$q_e = \frac{(C_0 - C_e)}{m} \times V \tag{1}$$

The percentage of the dye removal was calculated using the following equation

$$Removal\ (\%) = \frac{C_0 - C_e}{C_0} \times 100 \tag{2}$$

where q_e is the amount of dye biosorbed at equilibrium (mg/g), Removal % is the biosorption yield, C_0 and C_e are the initial and equilibrium liquid phase concentrations of dye (mg/L), V is the volume

of the dye solution (L) and m is the mass of biosorbent used (g).

2.6. Effect of salt ionic strength on dye biosorption

The study on the effect of salt ionic strength on the biosorption of MB and MG onto CPW are indispensable since the dyeing effluent usually composed of the high concentration of salt. The effect of salt concentration on the biosorption process of MB and MG was tested by the addition of different ionic strength of NaCl to the biosorption medium. About 50 ml of the dye solutions containing 10 mg/L initial dye concentration and ionic strength of NaCl (0.01–0.5 mol/L) with solution pH 10.0 for both MB and MG, respectively, agitated at 120 rpm and temperature of 30 °C. After the contact time of 2 h, the concentrations of MB and MG were analyzed to check the percentage removal of dyes by CPW.

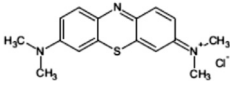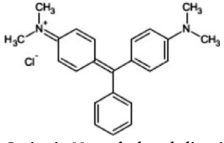## 2.7. Desorption and regeneration experimental procedure

In order to check the reusability of the CPW, exploration on the desorption and regeneration experiments was performed. The dye loaded biomass after the bisorption process in the optimal conditions was separated and dried in an oven. Then the dye loaded CPW was brought into contact with 50 ml of 0.1 M HCl used as the eluting agent. The desorption process was carried out for 2 h in a thermostated shaking incubator and the procedure are similar to that of the biosorption experiments conducted. After the desorption process, the CPW was washed thoroughly with distilled water for several times, and then oven dried. The regenerated CPW was analyzed for the reuse by subjecting for the further biosorption process. The biosorption followed with the desorption process were performed upto five cycles, to examine the MB and MG removal efficiency by CPW under the regenerated conditions.

3. Results and discussion

3.1. Characteristics of CPW

The physical and chemical characteristics of CPW was found, parameters and their respective values are presented in Table 2. The surface morphologies of the CPW were observed using the field emission scanning electron microscope at the two different magnifications of 6000× and 12,000× respectively. As seen in Fig. 1, the structure of CPW composed of rough, uneven, more number of cavities and irregular large pores. Such structural form of CPW provides large surface area that allows the easy accessibility for the biosorption of dyes. The

Table 1
General characteristics of methylene blue and malachite green.

Particulars	Methylene blue	Malachite green
Molecular structure		
Class	Cationic thiazine dye	Cationic N-methylated diamino triphenyl methane
Chemical formula	$C_{16}H_{18}N_3SCl$	$C_{23}H_{25}ClN_2$
Colour Index number	52,015	42,000
Colour Index name	Basic Blue 9 (BG 9)	Basic green 4 (BG 4)
Molecular weight (g/mol)	319.85	364.9
λ_{max} (nm)	664	619

Table 2
Characteristics of CPW.

Parameter	Value
Moisture content (%)	7.40
Volatile matter (%)	48.00
Ash content (%)	7.10
Fixed carbon (%)	37.50
Bulk density (g/cm^3)	0.50
Particle size (μm)	100–200
Point of zero charge	8.00
pH	7.35

XRD pattern of CPW was given in Fig. 2. The diffraction pattern of CPW showed two planes at 2θ near to 15° and 22°. The highest intensity of the peak was observed at 2θ of 22° corresponds to the (0 0 2) plane of cellulose. The weaker diffraction peak at 2θ of 15° was assigned to the contents of lignin and hemicellulose, which contribute to the amorphous nature of lignocellulosic biomass CPW [50].

The CPW is a lignocellulosic material mainly composed of cellulose, hemicellulose and lignin, which contribute to the distribution of various functional groups like hydroxyl, carboxyl, sulfhydryl, aldehydes and ketones on the biosorbent surface. The FT-IR analysis used to identify the characteristic functional groups of the biosorbent responsible for the removal of dyes from the aqueous solutions. The FT-IR spectra of CPW (Fig. 3a) showed several peaks suggested the poly functional nature of the biosorbent. Fig. 3b and c illustrates the FT-IR spectra of MB and MG biosorbed CPW.

In Fig. 3a, there exists a broad band between 3700 and 3000 cm^{-1} indicated the –OH stretching vibrations revealed that the surface of CPW has a higher number of alcoholic and phenolic –OH functional groups [51]. The peak assigned at 2926 cm^{-1} corresponds to the symmetric and asymmetric C–H stretching of –CH and CH functional groups in the lignin of CPW. The peak observed at 1737 cm^{-1} indicated the stretching of C = O functional group from lactones and quinones. The functional group –C = O from the stretching of amid-I band in the protein peptide bond was observed at 1622 cm^{-1} [52]. COO − peak appeared at 1424 cm^{-1} represented the carboxylate functional group. The peak located at 1319 cm^{-1} denoted the C–N stretching vibrations. The peak at 1251 cm^{-1} indicated the bending modes of functional groups O–C–H, C–C–H and C–O–H. A strong band around 1050 cm^{-1} confirmed the functional group C–O–C from the cellulose and lignin structures of CPW. A broad band appeared near 608 cm^{-1} corresponds to the stretching of C–Cl functional group [53,54].

Characteristic changes were observed in the FT-IR spectra of dye loaded CPW. The band of the stretching vibration of bonded hydroxyl groups was shifted from 3393 cm^{-1} to 3413 cm^{-1} and 3402 cm^{-1} for the MB and MG loaded CPW. The C = O stretching vibration at 1737 cm^{-1} and –C = O stretching from amid-I band at 1622 cm^{-1} of CPW shifted to 1745 cm^{-1} and 1633 cm^{-1} in the MB biosorbed CPW. A minor peak shift in the functional group region of C–N stretching vibrations and the bending vibrations of O–C–H, C–C–H and C–O–H were

observed in MB loaded CPW compared to CPW. Higher peak shift was seen from C–O–C stretching vibrations at 1059 cm^{-1} of CPW to 1036 cm^{-1} MB interacted CPW. Moreover significant shift from the peak region at 608 cm^{-1} (CPW) corresponds C–Cl stretching to 662 cm^{-1} (CPW loaded MB) and 661 cm^{-1} (CPW loaded MG) was observed. The predominant peaks from the FT-IR spectra of CPW before and after MB, MG biosorption were mentioned in the Table 3. The presence of vital functional groups from CPW might responsible for the effective interaction with the MB and MG dyes.

3.2. Effect of initial pH

The initial pH of the aqueous solution is a critical parameter in the process of biosorption, since it affects the biosorbent surface charges, the degree of ionization and the speciation of biosorbate. In order to investigate the influence of initial solution pH on the biosorption of MB and MG onto CPW, experiments were performed in the pH range of 2.0–10.0 at initial dye concentration of 10 mg/L. Fig 4 illustrated that the removal of MB and MG from aqueous solution highly dependent on the initial pH. The initial solution pH has influence on the functional groups such as hydroxyl, carbonyl and amine groups distributed on the CPW surface [55]. The biosorption capacity of CPW for the removal of MB and MG was found increased from 0.66 to 4.72 mg/g (Fig. 4a) and from 3.60 to 8.07 mg/g (Fig. 4b) respectively for the initial pH increase from 2.0 to 10.0. The percentage removal of MB and MG by CPW remarkably increased from 13.25 to 94.25% (MB) and from 43.29 to 96.94% (MG) respectively for the initial solution pH increase. For the biosorption of cationic dyes MB and MG using CPW, the maximum removal was attained at the initial solution pH of 10.0, represented that the biosorption of both dyes are highly dependent on the initial solution pH. At the low pH values, the dye removal by biosorbent showed decreased effect because the acidic condition produces more H$^+$ ions in the aqueous solution. This results in the protonation of CPW surface, which in turn prevents biosorption of MB and MG onto the biosorbent due to the effects of electrostatic repulsion and the competition behavior exhibited between H$^+$ ions and cationic dyes for the biosorption sites. With an increase of the initial pH, the number of OH$^-$ increases and the number of H$^+$ decreases. A negatively charged surface of CPW favors the biosorption of cationic dyes MB and MG through the electrostatic force of attractions [56]. The effect of initial solution pH had a similar behavior in the biosorption of MB and MG using CPW.

A plot for the determination of the pH Zero Point Charge (pH$_{PZC}$) of CPW was showed in Fig. 5. The pH$_{PZC}$ value CPW was found almost 8.0. This value confirmed the ranges of optimal pH values for the biosorption of MB and MG from aqueous solutions. The pH$_{PZC}$ of CPW represented that the biosorbent surface positively charged at solution pH value less than 8.0 and negatively charge at the pH value of greater than 8.0, which favors the biosorption of cationic dye like MB and MG respectively. At the higher solution pH, the better interaction of cationic dye with negatively charged functional groups in the CPW surface may takes place according to the following forms
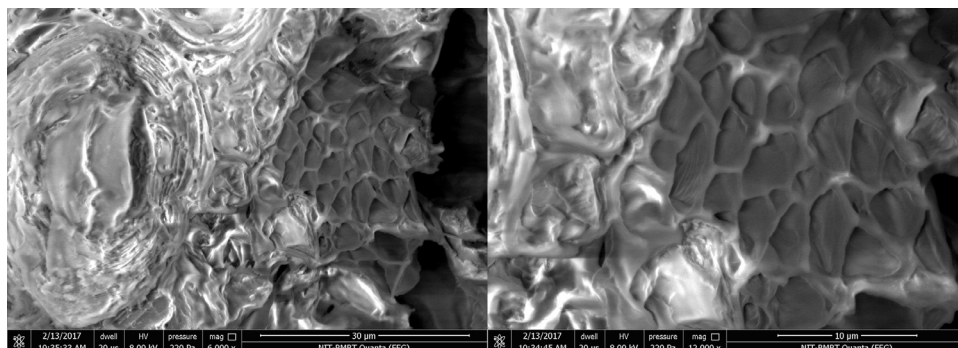
Fig. 1. The field emission scanning electron microscope images of CPW at two different magnifications.
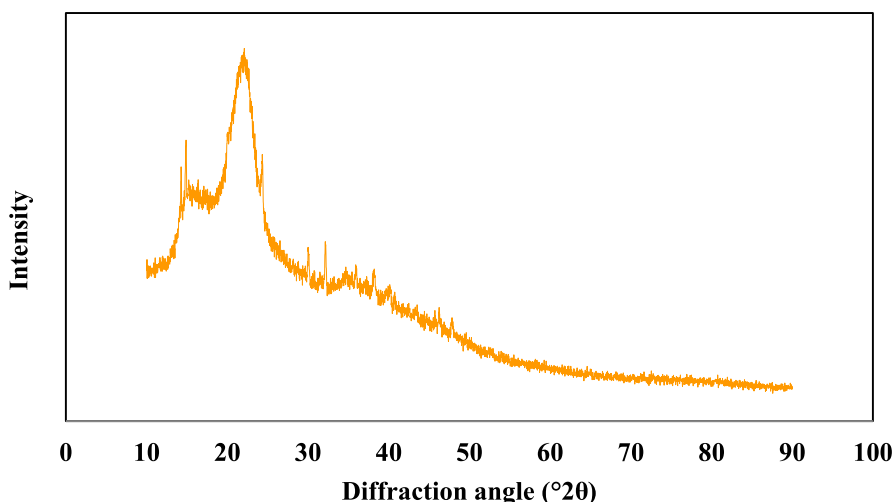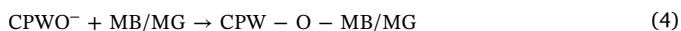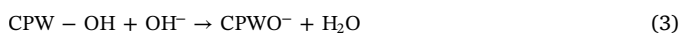
Fig. 2. X-ray diffraction pattern of CPW.

$$CPW - OH + OH^- \rightarrow CPWO^- + H_2O \tag{3}$$

$$CPWO^- + MB/MG \rightarrow CPW - O - MB/MG \tag{4}$$

Based on results from the effect of initial pH and pH_{PZC}, initial solution pH of 10.0 was selected for the biosorption of MB and MG from the aqueous solutions. Similar results were reported in the cationic dyes adsorption onto *Saraca asoca* leaf powder [57].

3.3. Effect of biosorbent dosage

Biosorbent dosage used to determine the removal capability of CPW towards the dye removal. The biosorption of MG and MB onto CPW was examined by varying the biosorbent dosage from 0.02 to 0.18 g at initial dye concentration of 10 mg/L and 10.0 initial pH. The values of biosorption capacity and the percentage removal of dyes for the different CPW dosage were shown in Fig. 6. The results indicated that the increase in the biosorbent dosage resulted in the increase of percentage removal from 70.75 to 94.50% (MB) and from 88.32 to 96.94% (MG), whereas the biosorption capacity of CPW showed decreased effect from 17.68 to 2.62 mg/g (MB) and from 22.08 to 2.69 mg/g (MG) respectively. The increase in the percentage removal with an increase in the biosorbent dosage was because of the more availability of the CPW surface area and the higher number of binding sites on the CPW. The biosorption capacity was found lesser at the higher CPW dosage, this was due to unsaturated biosorbent sites at a fixed concentration of the dyes and the biosorbent aggregation leads to the decrease in the biosorbent total surface area and increase in diffusional path length [58]. The results on the CPW biosorbent dosage effect on the removal of dyes are reliable with the previous results reported in the literatures [59]. The maximum removal efficiency was observed using the CPW biosorbent dosage of 0.1 g for MB and 0.06 g for MG, therefore the tested optimal biosorbent dosage was selected for the successive experiments of the biosorption study.

3.4. Effect of initial dye concentration

The initial dye concentration in the range of 10–50 mg/L was studied for the assessment of dye biosorption at CPW dosage of 0.1 g for MB, 0.06 g for MG and initial pH 10.0. Fig. 7 represents the biosorption capacity, percentage dye removal versus the different initial dye concentrations. By increasing the initial dye concentration, the biosorption capacity was found increased from 4.72 to 21.62 mg/g (MB) and from 8.05 to 37.50 mg/g (MG), but observed the decrease in the percentage dye removal from 94.50 to 86.50% (MB) and 96.70 to 90.00% (MG) respectively. [60, 61]. At the lower initial concentrations of the MB and MG removal, the ratio of the dye molecule to the biosorbent sites on

CPW was higher and most of the dye molecules undergoes better interaction with the biosorbent binding sites, hence resultant to the higher percentage of dye removal. With an increase in the initial concentrations of both the dyes, gradual decrease in the percentage removal of dye was observed and this was due to the saturation of CPW biosorption sites [62]. The biosorption capacity of CPW was increased towards the MB and MG removal for the increase in initial dye concentrations and this may be attributed due to the equilibrium process. The increase of dye concentration from 10 mg/L to 50 mg/L considered in the present study offered vital driving force to overcome the mass transfer resistance exhibited between CPW phase and the aqueous solution, consequent to the higher probability of collision between the dye molecules and the CPW binding sites [63].

3.5. Effect of contact time

The results of the experiment carried out to determine the equilibrium time for the biosorption of MB and MG onto CPW are represented in Fig. 8a and b. It was observed that the rapid biosorption of both dyes was happened in the initial period of the biosorption process, then the rate of biosorption gradually become slower attained almost constant value and referred to the equilibrium point. The fast biosorption of MB and MG occurred within the first 10 min of the biosorption process, then the biosorption rate towards dyes removal become slower and reached almost equilibrium around 100 and 120 min for all the studied concentrations of MB and MG respectively. The results are due to the fact that at the initial stage of the biosorption process, there was more accessibility of dye molecules in the unoccupied biosorbent surface active sites. With an increase of the time of the biosorption process, there was decrease in the biosorption sites for the residual dye molecules interaction. A similar dual trend was reported in the literature on the cationic dye removal [64].

3.6. Effect of temperature

In order to study the effect of temperature on the biosorption of MB and MG dyes on CPW, the experiments were carried out at the temperatures of 303, 313 and 323 K for the different initial dye concentration and at an initial solution pH 10.0. Fig. 9a and b illustrates the temperature dependent behavior on the biosorptive removal of MB and MG from aqueous solutions using CPW. The biosorption capacities of CPW and the percentage dye removal were recorded higher for the increase in initial dye concentrations from 10 to 50 mg/L at the temperature of 313 and 323 K. The Temperature has direct affect on the biosorption process since it affects the diffusion rate of the dye molecules by reducing the viscosity of the aqueous solutions and through
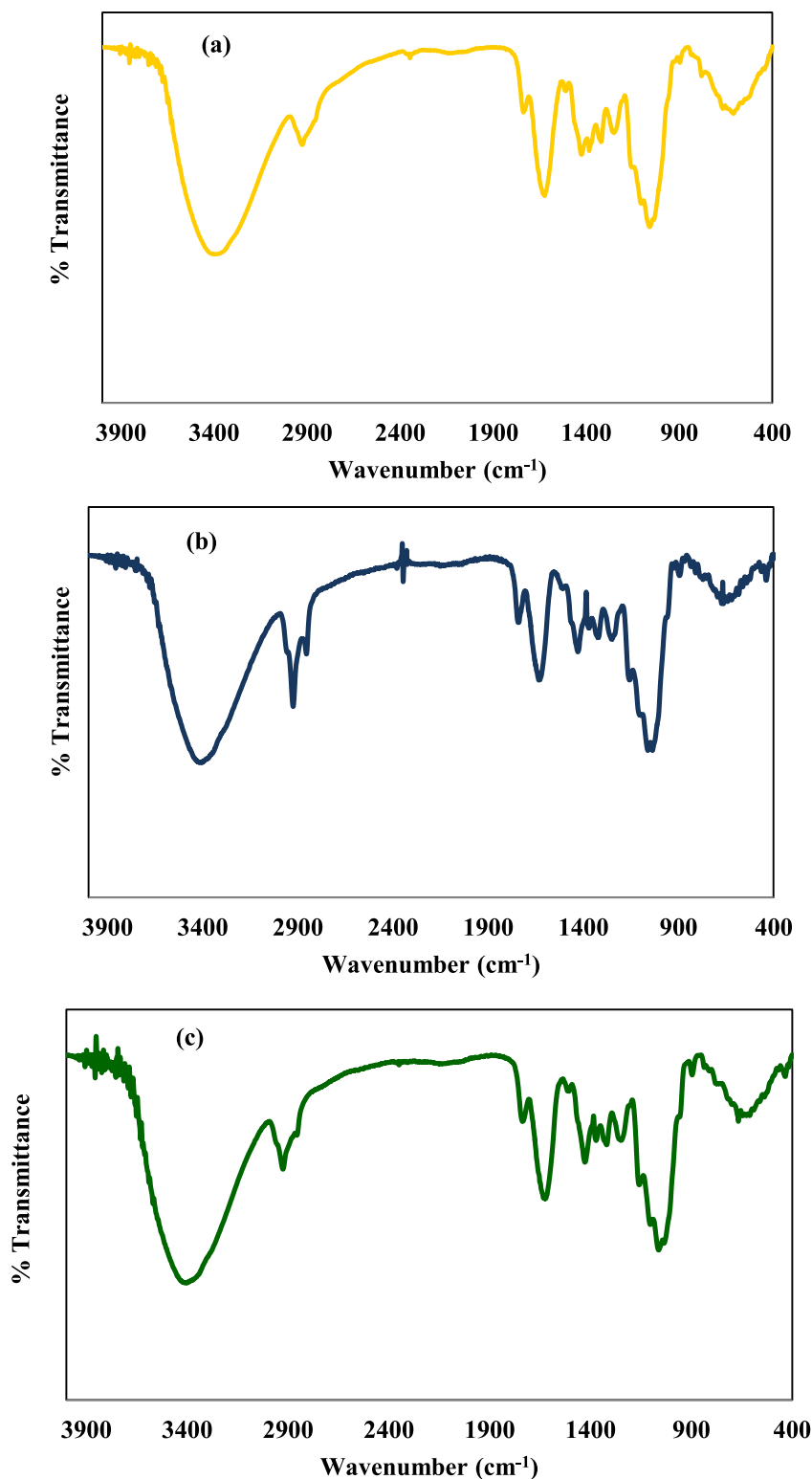
Fig. 3. FT-IR spectra of (a) CPW, (b) MB loaded CPW and (c) MG loaded CPW.

raising the number of the biosorption sites on the surface of CPW. Similar types of results were observed for the biosorption of dye at various temperatures [65,66]

3.7. Biosorption isotherm studies

Biosorption isotherms models used to illustrate the biosorbent interaction with the biosorbate and provide the relationship between the biosorption capacity and the liquid phase concentration of biosorbate under equilibrium condition at constant temperature. The most appropriate correlations of the biosorption equilibrium data are needed to optimize the design of the biosorption system for the dye removal [67]. Biosorption isotherm models provide the fundamental physicochemical data, used to evaluate the applicability of biosorption process. Each isotherm model characterized by certain constants, which provides significant information on the biosorbent surface properties, biosorbent affinities towards biosorbate, removal mechanisms and the uptake capacity of the biosorbent [68]. In order to understand the nature of

Table 3
Wave number (cm^{-1}) of the FT-IR spectra from CPW, MB loaded CPW and MG loaded CPW.

CPW	MB loaded CPW	Differences	MG loaded CPW	Differences	Functional groups
3393	3413	−20	3402	−9	Surface –OH stretching
2926	2924	2	2925	1	Aliphatic C–H stretching
1737	1745	−8	1737	–	Stretching of C = O
1622	1633	−11	1626	−4	–C = O stretching of amid-I band
1424	1428	−4	1428	−4	COO– in carboxylate
1319	1327	−8	1319	–	C–N stretching vibrations
1251	1245	6	1248	3	Bending vibrations of O–C–H, C–C–H and C–O–H
1059	1036	23	1061	−2	C–O–C stretching vibrations
608	662	−54	661	−53	Stretching of C–Cl
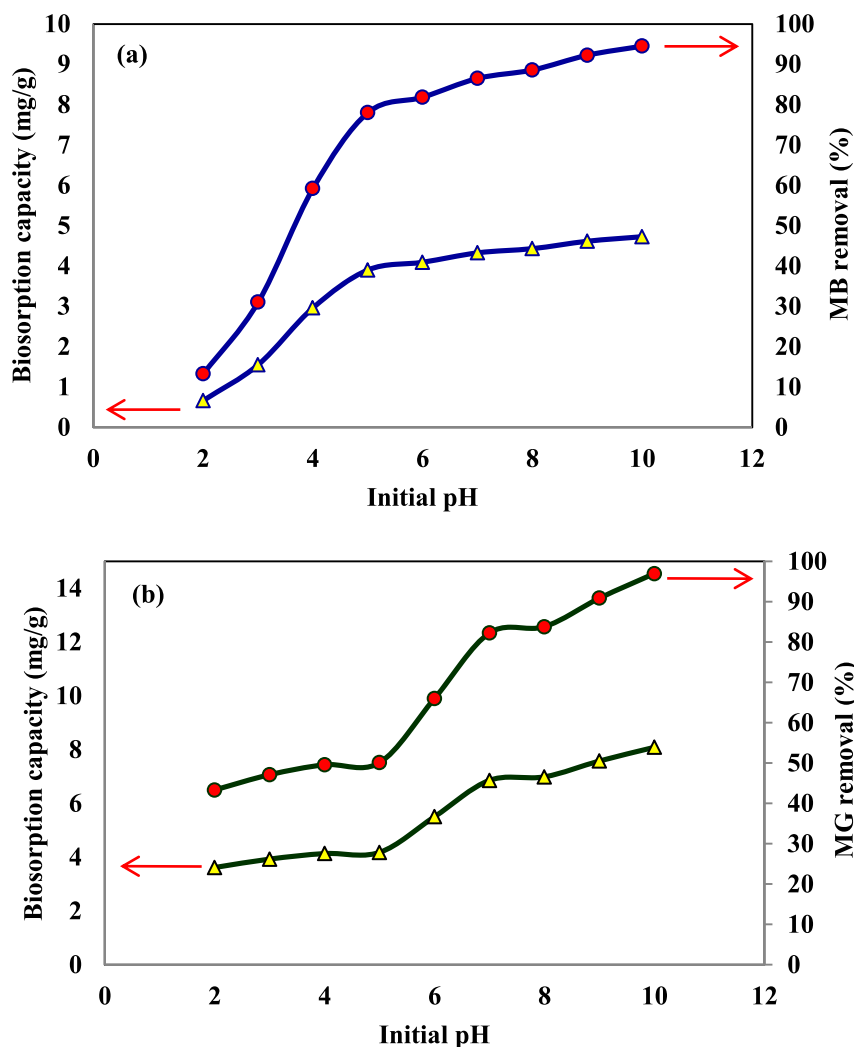
Fig. 4. Effect of initial pH on the biosorption capacity and the percentage removal of (a) MB and (b) MG using CPW.

interaction between CPW and dyes, the different isotherm models like Langmuir, Freundlich, Dubinin–Radushkevich, Temkin, Jovanovic, Halsey and Flory–Huggins were employed in the present study.
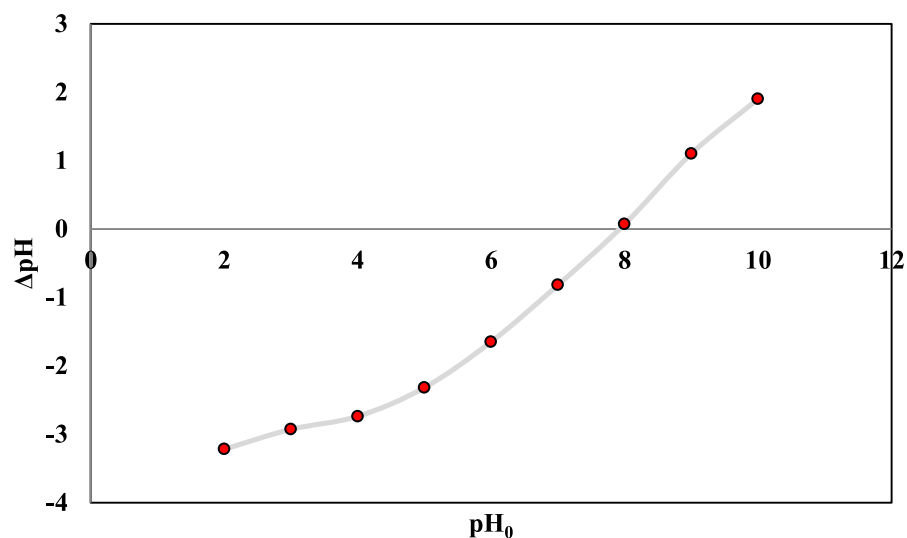
3.7.1. The Langmuir model

Langmuir isotherm was the first theoretically examined model in the adsorption of gases onto the solid surfaces. The Langmuir isotherm model represents the equilibrium distribution of biosorbate between the biosorbent and aqueous solution. The Langmuir model is the most widely used isotherm for the investigation of dye biosorption from liquid solution The Langmuir model provides information on biosorption capacity of the biosorbents. The model based on the assumption that the biosorption process occurs on a homogeneous surface through

monolayer formation without any interaction with the biosorbed molecules. Further, all the biosorption sites have equal biosorbate affinity and the biosorption at one site of the biosorbent will not affect the biosorption at the adjacent sites [69]. The Langmuir isotherm model of the following form was applied to the biosorption equilibrium at different concentrations

$$q_e = \frac{Q_0 K_L C_e}{1 + K_L C_e} \tag{5}$$

where C_e represent the equilibrium concentration of dye, q_e indicate the amount of dye biosorbed per unit mass of biosorbent at equilibrium. The Q_0 is the quantity of dye required for the monolayer formation on the unit mass of biosorbent (mg/g) and K_L denote the Langmuir

constant related to the energy of biosorption (L/mg).

One of the feature of the Langmuir isotherm model can be expressed in terms of a dimensionless constant [70], also known as separation factor (R_L) expressed as follows:

$$R_L = \frac{1}{1 + K_L C_0} \tag{6}$$

where C_0 represents the initial dye concentration (mg/L) and K_L denote the Langmuir constant (L/mg). If the value of R_L lies between 0 and 1 indicate the favorable biosorption, whereas the value of R_L greater than
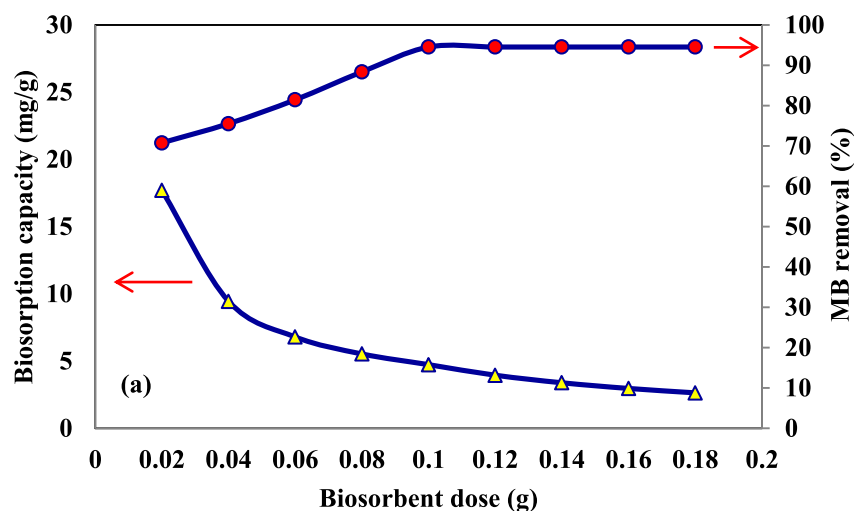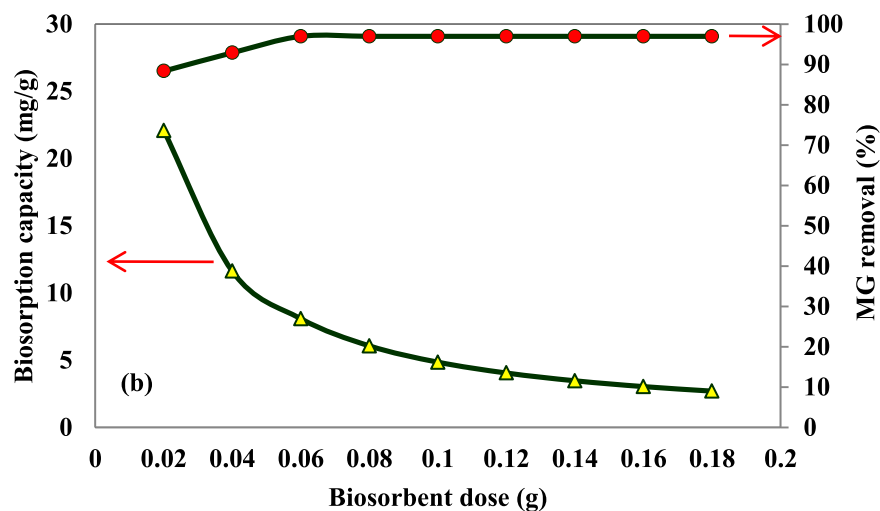

Fig. 6. Effect of biosorbent dosage on the removal of (a) MB and (b) MG using CPW.
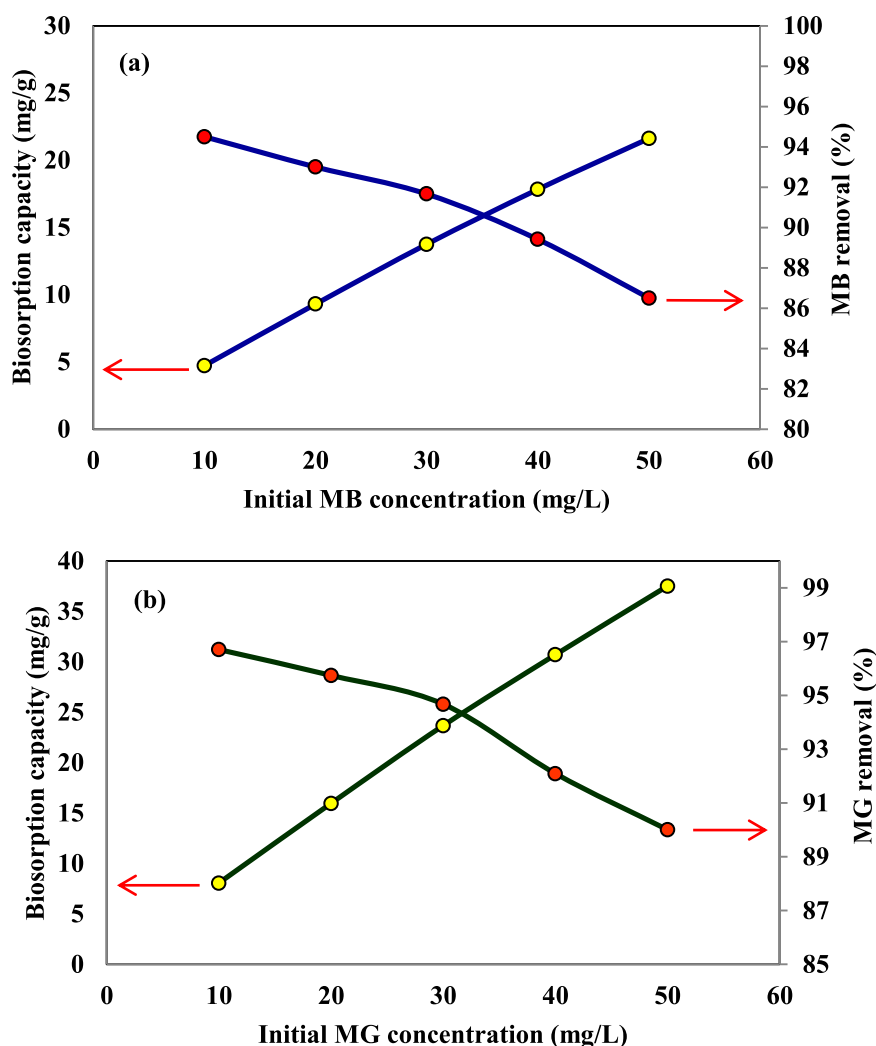
Fig. 7. Effect of (a) initial MB concentration and (b) initial MG concentration on biosorption capacity and percentage removal of dyes from aqueous solutions using CPW.

1 represent the unfavorable biosorption, R_L value equal to 1 denote the linear biosorption and the biosorption process indicate irreversible if the value of R_L equal to zero.

The Langmuir isotherm models constants Q_0 and K_L for the MB and MG biosorption were estimated from the intercept and slope of the linear plot of C_e/q_e versus $1/C_e$. Fig. 10 showed the linear plots of the Langmuir isotherm model for both the dyes. The experimental data fitted to the Langmuir isotherm model showed that the higher coefficient of determination value of 0.998 and 0.995 (Table 4) was obtained for MB and MG removal using CPW, demonstrated the best description of the biosorption experimental data using Langmuir model. The maximum biosorption capacity of CPW for the removal of MB and MG was found as 32.25 and 52.63 mg/g respectively. The separation factor for the different initial concentration of MB and MG was determined using the Eq. (6) and illustrated in Fig. 11. The separation factor values for the dyes biosorption towards were found in the range of 0.0292–0.0059 (MB) and 0.0501–0.0104 (MG). The results of separation factor showed that all the values are between 0 and 1 indicated favorable biosorption of MB and MG onto CPW.

3.7.2. The Freundlich model

The Freundlich model [71] represents the empirical equation, based on the biosorption of heterogeneous energetic distribution of active sites accompanied by interactions between biosorbed molecules. The Freundlich isotherm model suggests the multilayer biosorption. The model considers the assumption that logarithmic decrease in the

biosorption enthalpy with an increase in the fraction of occupied sites on the biosorbent. The non-linear form of the model commonly given by:

$$q_e = K_F C_e^{1/n_F} \qquad (7)$$

where K_F denote the biosorption capacity related to the bonding energy (L/g) and n_F is the heterogeneity factor indicate the deviation from biosorption linearity, also known as Freundlich isotherm model coefficient. From the plot of $\log(q_e)$ versus $\log(C_e)$, the slope and intercept gives the values of Freundlich isotherm constants $1/n_F$ and K_F, presented in Table 4. The value of $1/n_F$ obtained from the Freundlich isotherm model for the removal of MB and MG was found less than one, represented that the dyes removal using CPW are favorability of biosorption. Furthermore, the K_F magnitude of 7.24 (MB) and 16.33 (MG) indicated high biosorption capacity and easy uptake of dye molecules from aqueous solutions by CPW.

3.7.3. The Dubinin–Radushkevich model

The Dubinin–Radushkevich isotherm model [72] estimates the porosity apparent free energy and the biosorption characteristics. This isotherm model is dependent on the temperature of the biosorption, used in the prediction of the nature of biosorption process through the determination of the mean free energy of biosorption. The Dubinin–Radushkevich isotherm model dose not assumes a homogeneous surface or a constant biosorption potential. The non linear form of this model given by the following equation
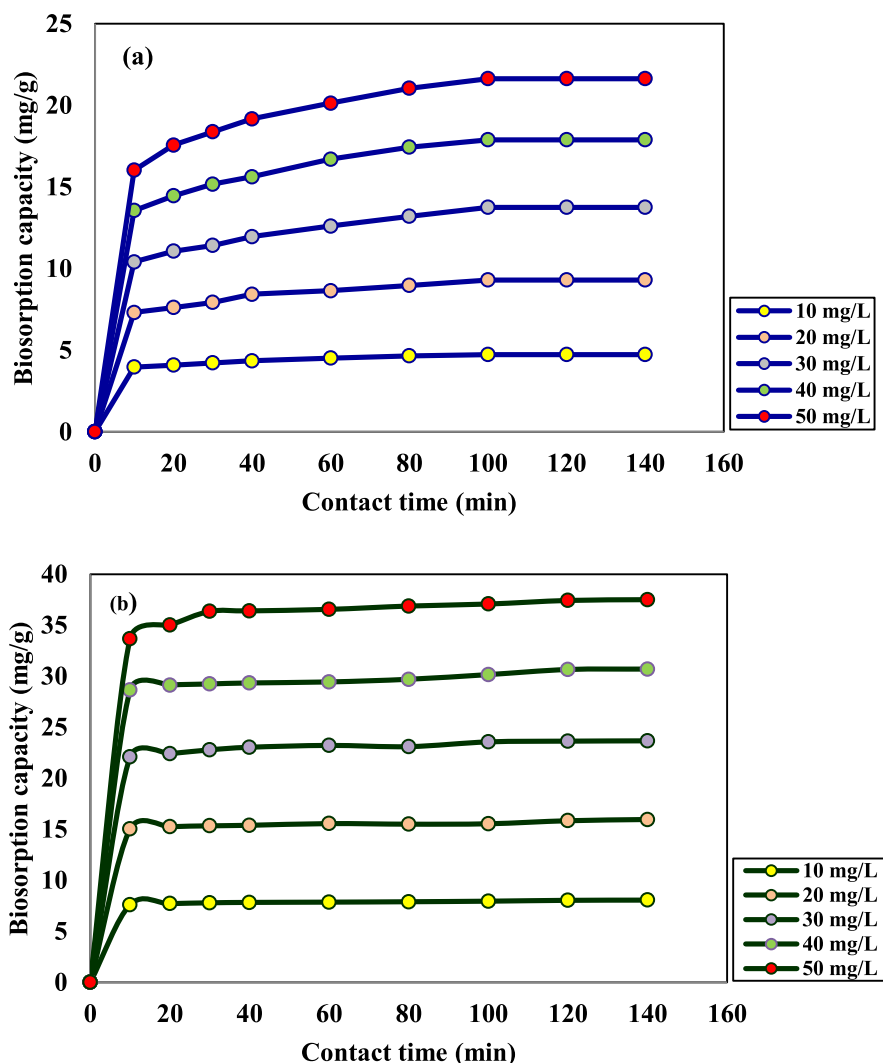
Fig. 8. Effect of contact time on the biosorption of (a) MB and (b) MG using CPW for different initial dye concentrations.

$$q_e = Q_m exp^{-K\varepsilon^2} \tag{8}$$

$$\varepsilon = RT \ln\left(1 + \frac{1}{C_e}\right) \tag{9}$$

where Q_m indicate the Dubinin–Radushkevich maximum biosorption capacity (mg/g), K symbolize the activity coefficient related to biosorption mean free energy (mol²/J²). ε represent the Polanyi potential. R denote the universal gas constant (8.314 J/mol K) and T is the temperature (K).

The mean biosorption energy E (kJ/mol), defined as the free energy change when one mole of molecule transferred from infinity in the aqueous solution to the biosorbent surface. The equation relating the mean biosorption energy and activity coefficient represented in the following equation.

$$E = \frac{1}{\sqrt{2K}} \tag{10}$$

The value of mean biosorption energy provides important information regarding the type of biosorption process. Biosorption process controlled by means of chemical mechanisms, when the value of E lies in the range from 8 to 16 kJ/mol. The physical mechanisms govern on the biosorption process, when the value of E less than 8 kJ/mol.

The values of Q_m and K were determined from the plot of $\log(q_e)$ versus ε^2. The maximum biosorption capacity Q_m found using Dubinin–Radushkevich isotherm model for biosorption of MB and MG

using CPW was 17.69 and 31.15 mg/g, these values are not closer to that of the Langmuir isotherm model predicted biosorption capacity (Table 4). The value of mean biosorption energy for MB and MG are less than 8 kJ/mol, interpreted that the biosorption of both onto CPW was based on physical biosorption. The coefficient of determination obtained from Dubinin–Radushkevich model are lesser than those obtained for the Langmuir and Freundlich isotherm models represented the invalid of this model for describing the biosorption of MB and MG using CPW.

3.7.4. The Temkin model

The Temkin isotherm model [73] includes the interactions of the biosorbent–biosorbate. The model relates the effects of heat of biosorption that decreases linearly with the biosorbate and the biosorbent surface interactions at moderate values of the biosorbate concentrations. The model considers the assumption that the fall in the heat of biosorption is linear rather than logarithmic, as implied in the Freundlich isotherm. The Temkin isotherm model represented in the non linear form using the following relation

$$q_e = B_T \ln(A_T C_e) \tag{10a}$$

where, $B_T = (RT)/b_T$, T is the absolute temperature in K and R is the universal gas constant (8.314 J/mol K). b_T denote the Temkin isotherm constant related to the heat of biosorption (kJ/mol), A_T represent Temkin isotherm equilibrium binding constant (L/g). A plot of q_e versus $\ln(C_e)$ at a constant 303 K was used to calculate the Temkin isotherm
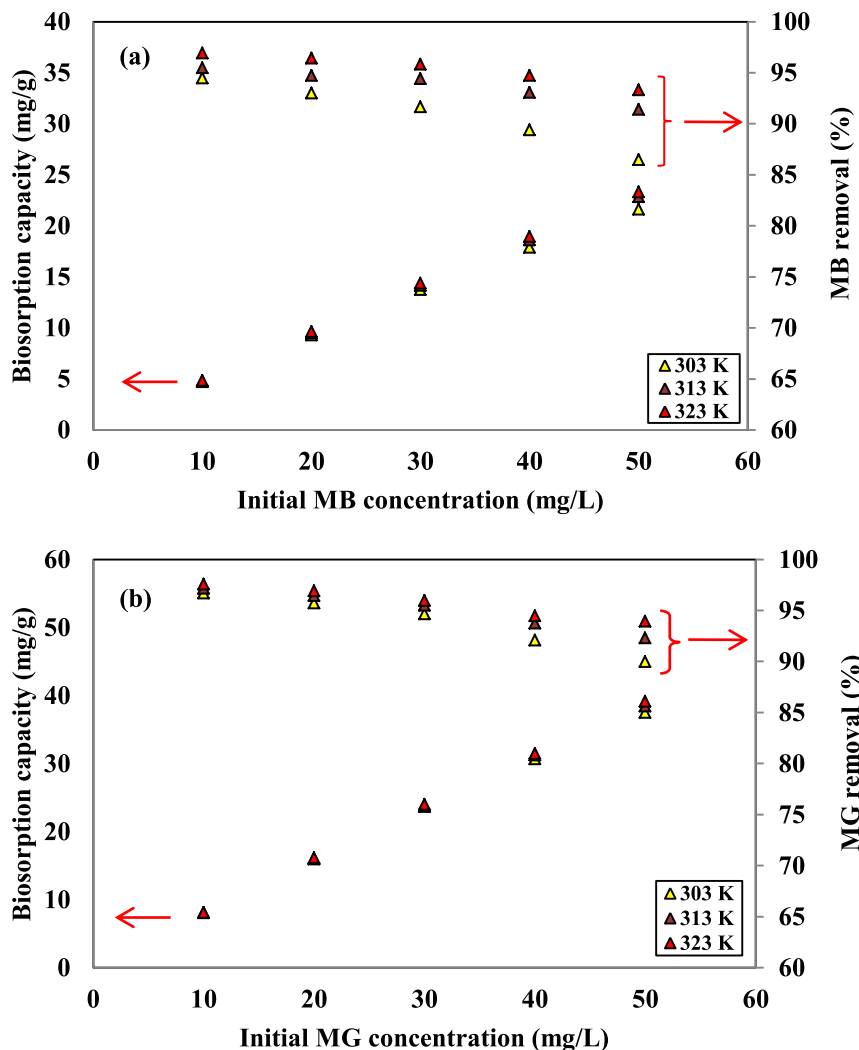
Fig. 9. Effect of temperature on the removal of different initial concentrations of (a) MB and (b) MG from aqueous solutions using CPW.

constants. The calculated constants values of Temkin isotherm model are mentioned in Table 4. The obtained coefficient of determination value for Temkin isotherm model was 0.987 (MB) and 0.991 (MG) confirmed the better fit of biosorption equilibrium data than Dubinin-Radushkevich isotherm, but not good fitting as compared to the Langmuir isotherm model.

3.7.5. The Jovanovic model

The Jovanovic [74] isotherm model assumptions are similar to that contained in the Langmuir model, in addition the model takes into account of some mechanical contacts between the biosorbent and biosorbate molecules. The Jovanovic isotherm indicate as the another model for the estimation of monolayer localized biosorption without
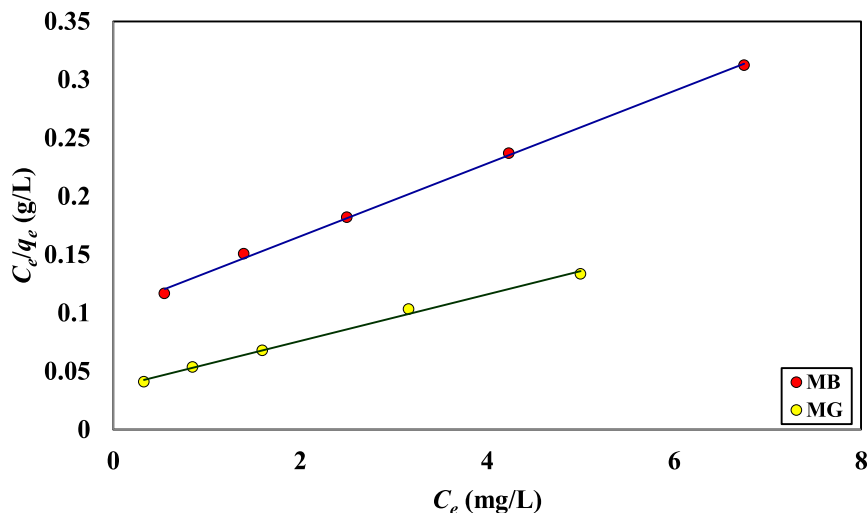

Fig. 10. Langmuir isotherm plots for the biosorption of MB and MG onto CPW.

Table 4
Isotherm model parameters for the biosorption of MB and MG onto CPW.

Isotherms	Values	
	MB	MG
Langmuir		
Q_o (mg/g)	32.25	52.63
K_L (L/mg)	3.3226	1.8947
R^2	0.998	0.995
Freundlich		
KF (L/g)	7.24	16.33
nF	1.6313	1.7857
R^2	0.987	0.980
Dubinin–Radushkevich		
Qm (mg/g)	17.69	31.15
K (mol^2/J^2)	2×10^{-7}	1×10^{-7}
E (kJ/mol)	1.5811	2.2360
R^2	0.902	0.924
Temkin		
A_T (L/g)	3.2332	5.8096
b_T (kJ/mol)	0.3697	0.2339
R^2	0.987	0.991
Jovanovic		
q_{mj} (mg/g)	6.02	10.96
K_j (L/g)	−0.095	−0.122
R^2	0.800	0.776
Halsey		
K_H	0.0395	0.0068
n_H	−1.6313	−1.7857
R^2	0.987	0.980
Flory–Huggins		
K_{FH}	0.0003	0.0006
n_{FH}	−1.857	−1.415
R^2	0.946	0.929

lateral interactions. In addition, the Jovanovic model extended to the heterogeneous surface as a semi-empirical model in the form of Jovanovic–Freundlich model. The Jovanovic isotherm model is given by the following equation

$$q_e = q_{mj}\left(1 - e^{(K_j C_e)}\right) \tag{11}$$

where q_{mj} denotes the maximum biosorption capacity predicted using the Jovanovic isotherm model (mg/g), K_j represent the Jovanovic isotherm model constant (L/g). The Jovanovic biosorption isotherm model constants for the dyes biosorption was calculated using the linear plot of log(q_e) versus C_e. The maximum biosorption capacities for the studied dyes according to this model were found lower than the Langmuir maximum monolayer biosorption capacities (Table 4). Moreover, the coefficient of determination values for this model towards MB and MG removal was 0.800 and 0.776, observed least fitted to the experimental

data compared to the other biosorption isotherm models considered in the present investigation.

3.7.6. The Halsey model

The Halsey [75] biosorption isotherm model explains about the multilayer biosorption process, which attests the heteroporous nature of the biosorbent. The non-linear form of the Halsey isotherm model represented in the following equation

$$q_e = \exp\left(\frac{\ln K_H - \ln C_a}{n_H}\right) \tag{12}$$

where K_H represent the Halsey isotherm constant, n_H indicate the Halsey isotherm model exponent. The Halsey isotherm model constants were obtained from the plot of ln(q_e) versus ln(C_e). The coefficient of determination value for the biosorption of MB and MG was found as 0.987 and 0.980 (Table 4) and represented that the Halsey model better fitted than the Dubinin–Radushkevich and Jovanovic isotherm models.

3.7.7. The Flory–Huggins model

The Flory–Huggins [76] isotherm model account for the degree of surface coverage characteristics of biosorbate onto the biosorbent. The expression of Flory–Huggins model mentioned as follows

$$\frac{Q}{C_0} = K_{FH}(1 - Q)^{n_{FH}} \tag{13}$$

$$Q = 1 - C_e/C_0 \tag{14}$$

where Q denote the degree of surface coverage, K_{FH} represent the Flory Huggins isotherm model equilibrium constant of biosorption and n_{FH} indicate the model exponent, refers to the number of dye molecules occupying in the biosorption site. The Flory–Huggins isotherm model constants were found from the linear plot of log(Q/C_0) versus log (1 − Q). The low values of K_{FH}, negative values of n_{FH} and the lower coefficient of determination for both the dyes revealed the inapplicability of this model to describe the experimental data of dyes biosorption using CPW.

3.8. Biosorption kinetic studies

The biosorption kinetics provides insights over the dynamics of dye biosorption onto the biosorbent, moreover helps to examine the controlling mechanism of the biosorption process such as the chemical reaction, mass transfer and diffusion control. The kinetics describes about the biosorbate uptake by the biosorbent, which in turn controls the residence time of the biosorbate at the biosorbent–solution interface [77,78]. In order to investigate the controlling mechanism of the dyes
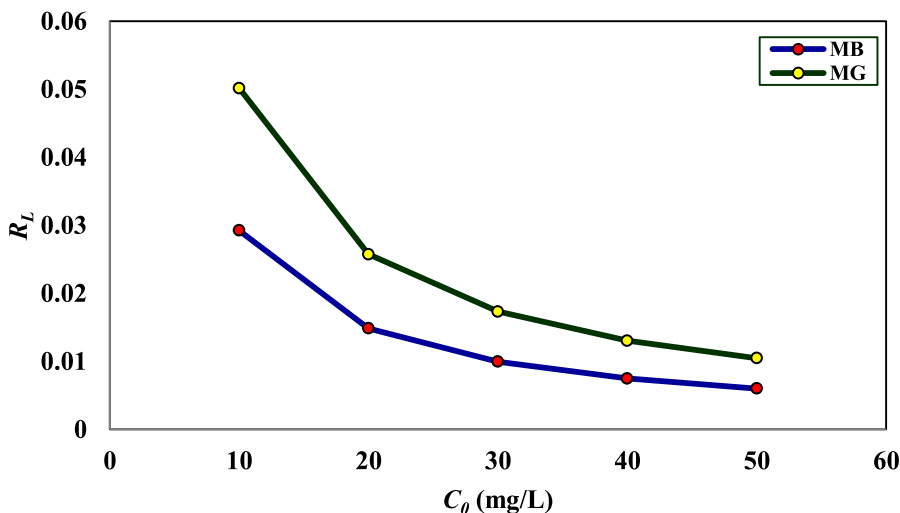
Fig. 11. Effect of initial dye concentration on dimensionless separation factor.

biosorption onto CPW, the experimental data were analyzed using four different kinetic models like pseudo-first-order, pseudo-second-order, Elovich and Intraparticle diffusion respectively.

3.8.1. Pseudo-first-order model

The Lagergren [79] proposed pseudo-first-order kinetic model, has its significance in the biosorption rate constant determination based on the biosorption capacity The pseudo-first-order kinetic model considered the assumption that the rate of change of the biosorbate removal with time leads to change in the biosorption capacity of the biosorbent. The linearized form of the pseudo-first-order kinetic equation expressed as follows:

$$\log(q_e - q_t) = \log q_e - \frac{k_1}{2.303}t \tag{15}$$

where q_e denote the biosorption capacity (mg/g) at equilibrium time and q_t indicate the biosorption capacity (mg/g) at any time, t (min), k_1 represent the pseudo-first-order kinetic model rate constant (1/min).

For the determination of the Lagergren pseudo-first-order kinetic constants, plots of $\log(q_e-q_t)$ versus t were made and the constant values q_e, k_1 were determined from the intercept and slope of the plot (Table 5). The values of the coefficient of determination for pseudo-first-order model were found lower for all the studied initial dye concentrations of both MB and MG. Therefore, the pseudo-first-order kinetic model failed to explain the biosorption of dyes onto CPW with poor fit at the various dyes concentrations.

3.8.2. Pseudo-second-order model

The Ho and Mckay [80] proposed the pseudo-second-order kinetic

model, predicts the biosorption behavior over the entire time of the biosorption process. The pseudo-second-order model based on the assumption that the biosorption follows chemisorption, occurs through the valence forces from electrons sharing between the dye and biosorbent functional groups. The mathematical expression of the pseudo-second-order kinetic equation represented in the following form

$$\frac{t}{q_t} = \frac{1}{k_2 q_e^2} + \frac{t}{q_e} \tag{16}$$

where k_2 indicate the rate constant of the pseudo-second-order kinetic model (g/mg min). In order to determine the pseudo-second-order rate constants, linear plots between t/q_t versus t were drawn and the constants values were obtained from the slope and intercept of the plots. Fig. 12a and b represents the pseudo-second-order kinetic plots for the biosorption of MB and MG onto CPW at various initial dye concentrations. The coefficient of determination values for the pseudo-second-order model for all the studied concentrations were near to unity for MB and MG biosorption, indicated that pseudo-second-order kinetic model best described the biosorption kinetics. The results are attributed to the fact of the chemisorption mechanisms as the rate determining step of the dyes biosorption process. The values of the pseudo-second-order kinetic model rate constant (k_2) decreased with an increase of the initial concentrations of both the dyes. These results revealed that the biosorption rate was decreased with the increase of initial concentrations of MB and MG.

3.8.3. Elovich model

The Elovich [81] model suitable to illustrate the biosorption performance concurs with the nature of chemical biosorption and

Table 5
Kinetic parameters for the biosorption of MB and MG onto CPW at various initial dye concentrations.

Kinetic models	Parameters	Values				
		Methylene blue (mg/L)				
Pseudo-first-order		10	20	30	40	50
	k_1 (1/min)	0.0414	0.0322	0.0322	0.0368	0.0368
	q_e (mg/g)	2.11	4.38	7.07	9.86	11.77
	R^2	0.878	0.853	0.872	0.911	0.911
		Malachite green (mg/L)				
	k_1 (1/min)	0.0299	0.0230	0.0391	0.0345	0.0345
	q_e (mg/g)	1.32	2.31	5.02	7.04	8.18
	R^2	0.712	0.571	0.816	0.716	0.806
Pseudo-second-order		Methylene blue (mg/L)				
		10	20	30	40	50
	k_2 (g/mg min)	0.0538	0.0188	0.0103	0.0086	0.0073
	q_e (mg/g)	4.87	9.70	14.49	18.86	22.72
	R^2	0.999	0.999	0.998	0.999	0.999
		Malachite green (mg/L)				
	k_2 (g/mg min)	0.1001	0.0468	0.0294	0.0176	0.0164
	q_e (mg/g)	8.13	16.12	24.39	31.25	38.46
	R^2	0.999	0.999	0.999	0.999	0.999
Elovich		Methylene blue (mg/L)				
		10	20	30	40	50
	α (mg/g min)	4558.59	380.23	176.92	261.176	253.625
	β (g/mg)	3.030	1.1737	0.7027	0.5446	0.4382
	R^2	0.973	0.973	0.974	0.979	0.987
		Malachite green (mg/L)				
	α (mg/g min)	2.13×10^{18}	1.33×10^{20}	3.17×10^{14}	3.25×10^{15}	1.70×10^{10}
	β (g/mg)	6.097	3.322	1.6393	1.3458	0.7485
	R^2	0.969	0.879	0.961	0.875	0.920
Intraparticle diffusion		Methylene blue (mg/L)				
		10	20	30	40	50
	k_{id} (mg/g min$^{0.5}$)	0.096	0.249	0.418	0.534	0.658
	C (mg/g)	3.70	6.62	9.22	12.19	14.64
	R^2	0.948	0.954	0.968	0.952	0.942
		Malachite blue (mg/L)				
		10	20	30	40	50
	k_{id} (mg/g min$^{0.5}$)	0.048	0.090	0.176	0.227	0.372
	C (mg/g)	7.49	14.79	21.70	27.92	33.46
	R^2	0.964	0.907	0.926	0.941	0.819

heterogeneous systems. The linearized form of the Elovich kinetic model represented as follows

$$q_t = \frac{1}{\beta} \ln(\alpha\beta) + \frac{1}{\beta} \ln t \qquad (17)$$

where α indicate the initial rate of biosorption (mg/g min) and β represent the Elovich constant, refers to the extent of surface coverage (g/mg). The constant values of the Elovich kinetic model are obtained from the plot of q_t versus $\ln(t)$ and represented in Table 5. The value of initial rate of biosorption (α) was higher at the lower initial dye concentration and the value of β decreased with an increase of the initial dye concentration. The coefficient of determination value of Elovich kinetic model for the biosorption of MB and MG using CPW was found lower than the pseudo-second-order kinetic model.

3.8.4. Intraparticle diffusion model

The biosorption of dyes from the aqueous solution onto the biosorbent occurs through the following steps, the biosorbate transport from bulk solution to the biosorbent outer surface through molecular diffusion, then the transport of biosorbate from the biosorbent outer surface into the interior sites and followed with the biosorption of dye molecules from the active sites into the interior surface of the biosorbent pores. The slowest step will be the rate determining step of the overall biosorption process [82]. The intraparticle diffusion model proposed by Weber and Morris [83] stated that in case of intraparticle diffusion the rate determining factor, the biosorption capacity varies with the square root of time according to the following expression.

$$q_t = k_{id} t^{0.5} + C \qquad (18)$$

where k_{id} denote the constant of intraparticle diffusion model (mg/g min$^{0.5}$) and C indicate boundary layer thickness (mg/g). The constants value of the intraparticle diffusion model was determined from the plots of q_t versus $t^{0.5}$ for dye biosorption using CPW. The constants values of this kinetics model are presented in Table 5. The boundary layer thickness (C) was increased with an increase in the initial dyes concentrations, which increases the resistance to the external mass transfer. The lines of the plots of intraparticle diffusion model for the MB and MG biosorption had nonzero intercept origin (figure not shown). These results indicated that the biosorption process might be of complex mechanism comprised of both surface biosorption and intraparticle diffusion [84].

3.9. Biosorption thermodynamic studies

The thermodynamics parameters such as the Gibbs free energy change (ΔG°), enthalpy change (ΔH°) and entropy change (ΔS°) used to examine temperature effects on the dyes removal using CPW. The thermodynamic parameters provide insights over the mechanism and behavior of the biosorption process. The thermodynamics parameters were evaluated using the following equations

$$\Delta G^\circ = -RT \ln K_d \qquad (19)$$

$$\ln K_d = \frac{\Delta S^\circ}{R} - \frac{\Delta H^\circ}{RT} \qquad (20)$$

$$\Delta G° = \Delta H° − T\Delta S° \qquad (21)$$

where K_d denote the distribution coefficient for biosorption, T indicate the absolute temperature (K) and R refers the universal gas constant (8.314 J/mol K). $\Delta G°$, $\Delta H°$ and $\Delta S°$ are the thermodynamic constants.

Using Eq. (19) the values of Gibbs free energy ($\Delta G°$) was found, the values of enthalpy change ($\Delta H°$) and entropy change ($\Delta S°$) values was determined from the plot of $\ln(K_d)$ versus $1/T$ (Fig. 13). The calculated thermodynamic constants values were presented in Table 6. Gibbs free energy change showed negative sign for MB and MG biosorption for initial dye concentrations of 10 to 50 mg/L, confirmed the feasible and spontaneous nature of dye biosorption. The decrease in the value of Gibbs free energy with increasing temperature represented that the biosorption of dyes onto CPW was more favorable at higher temperature. The values of enthalpy change were observed positive for the biosorption of dyes, for all the concentrations considered in this study. The results of the enthalpy change indicated that the dyes biosorption process was endothermic. The positive values of the entropy change revealed the conscious options of biosorbent raised with an increase of orderliness between the dye molecules and the biosorbent [85].

3.10. Effect of NaCl on the dyes biosorption

In the process of dying, salts are used and lead to their occurrence in the industrial wastewater. The concentration of the salts variation depends on the source and type of the industrial effluents [86]. The effect of NaCl concentration on the percentage removal of dyes using CPW
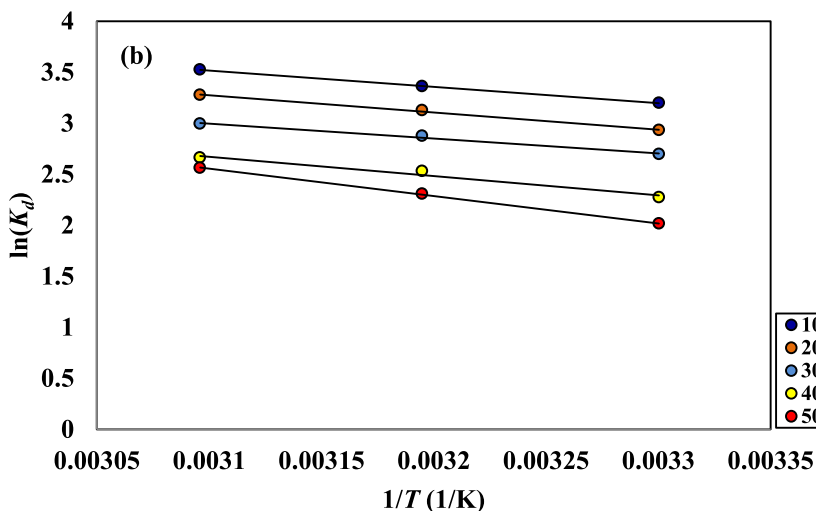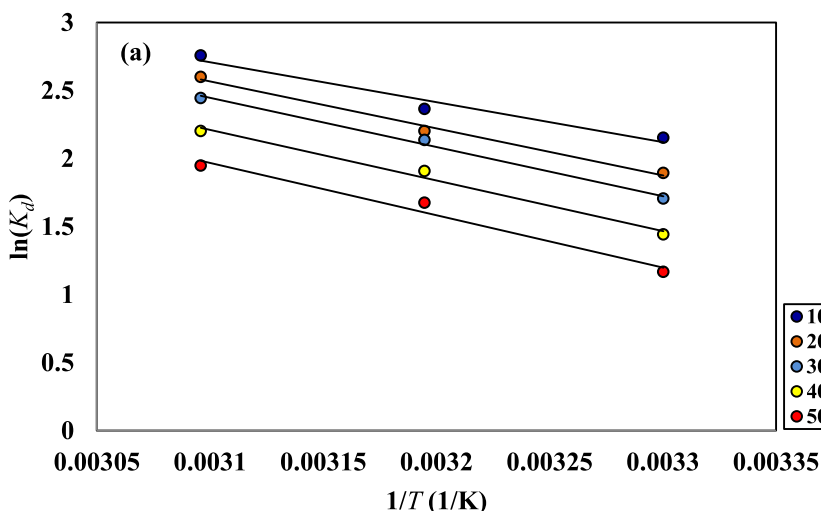
Table 6
Thermodynamic parameters for the biosorption of MB and MG onto CPW at different initial dye concentrations.

C_0(mg/L)	T (K)	MB			MG		
		$\Delta G°$ (kJ/mol)	$\Delta H°$ (kJ/mol)	$\Delta S°$ (J/mol K)	$\Delta G°$ (kJ/mol)	$\Delta H°$ (kJ/mol)	$\Delta S°$ (J/mol K)
10	303	−5.41	24.48	98.35	−8.05	13.31	70.54
	313	−6.14			−8.74		
	323	−7.39			−9.46		
20	303	−4.77	28.65	110.16	−7.38	13.97	70.55
	313	−5.72			−8.13		
	323	−6.98			−8.79		
30	303	−4.29	30.04	113.48	−6.78	12.13	62.52
	313	−5.55			−7.48		
	323	−6.55			−8.03		
40	303	−3.62	30.93	114.23	−5.72	15.78	71.13
	313	−4.96			−6.58		
	323	−5.90			−7.14		
50	303	−2.93	31.88	115.14	−5.07	22.21	90.04
	313	−4.35			−6.00		
	323	−5.22			−6.87		

was examined in the presence of increasing salt concentration from 0.01 to 0.1 M NaCl. The obtained results of the influence of NaCl concentration on the biosorption of MB and MG are illustrated in Fig. 14. The percentage dye removal decreased from 86.41 to 63.75% (MB) and
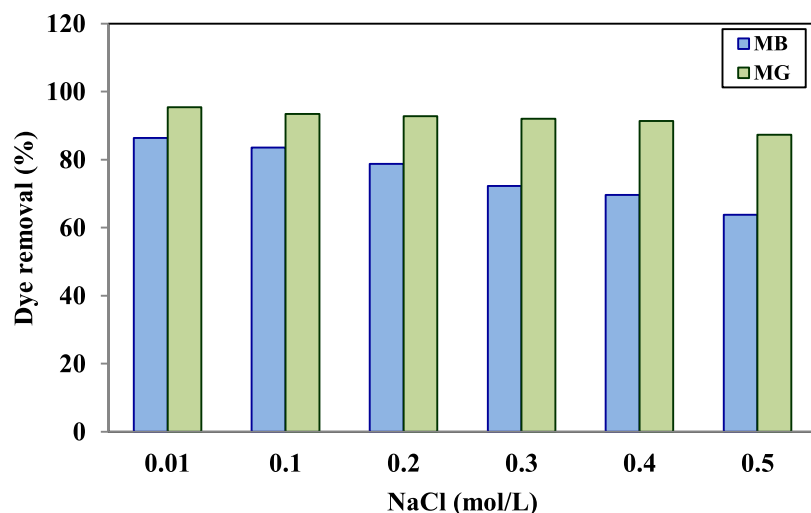

Fig. 13. The plots of $\ln(K_d)$ versus $1/T$ for the biosorption of (a) MB and (b) MG on CPW.

Fig. 14. Effect of NaCl concentrations on the biosorption of MB and MG onto CPW.

Table 7

Comparison of biosorption capacities of CPW with different biosorbents for the removal of MB and MG.

MB			MG		
Biosorbent	Biosorption capacities (mg/g)	References	Biosorbent	Biosorption capacities (mg/g)	References
Cereal chaff	20.30	[88]	Sugarcane dust	4.88	[95]
Posidonia oceanica	5.56	[89]	Tamarind fruit shell	1.95	[96]
Cashew nut shell	5.31	[90]	Rubber wood sawdust	36.50	[97]
Coconut coir dust	29.50	[91]	*Caulerpa racemosa* var. *cylindracea*	25.67	[98]
Azadirachta indica leaf powder	19.61	[92]	*Annona squmosa* seed	25.91	[99]
Acacia fumosa seed shell	1.85	[93]	Banana pseudo-stem fiber	26.50	[100]
Scenedesmus dimorphus	6.00	[94]	*Daucus carota* stem powder	43.40	[101]
Carica papaya wood	32.25	Present study	*Carica papaya* wood	52.63	Present study

95.38 to 87.30% (MG) for the increase in the salt concentration from 0.01 to 0.1 M NaCl. The presence of the higher concentration of NaCl significantly affected MB removal efficiency and in case of the MG removal, comparatively slight decrease in the removal efficiency was observed. The decrease in the removal efficiency of the MB and MG may be attributed to the competitive effect exhibited between cationic dyes (MB and MG) and Na$^+$ cations for the biosorption sites on the CPW. Moreover the possibility of increased ionic strength might had decreased the activity of cationic dyes and the biosorbent active sites, caused the decrease in the removal efficiency of the dyes. Previous researchers reported that considerable decrease in the dye biosorption

occurred due to the presence of NaCl in the biosorption medium [87].

3.11. Desorption and regeneration studies

Biosorbent regeneration aspects are vital in economic point of view and for the feasible biosorption process. For the desorption assessment of the dye loaded CPW, 0.1 M HCl was used as the desorbing agent. The reusability of CPW for the five successive cycle's dyes biosorption was represented in Fig. 15. The percentage MB removal in the first cycle showed 94.08% and 84.41% in the fifth cycle. The regeneration investigation of MG biosorption showed that negligible decrease in the
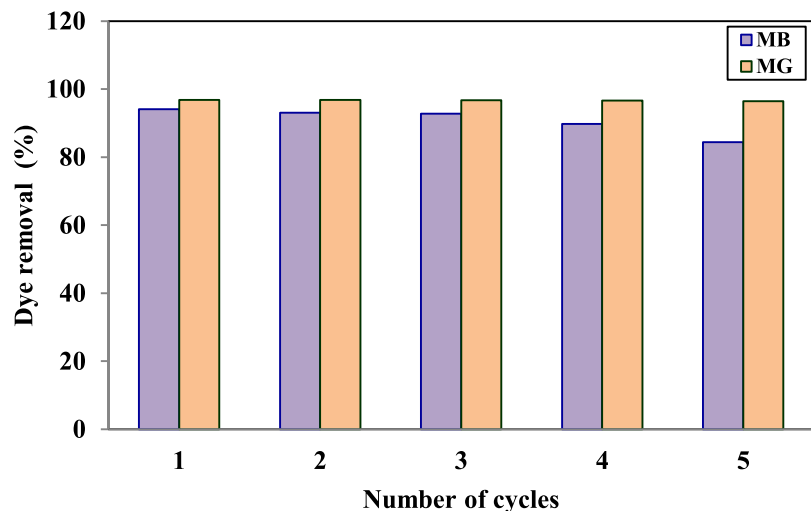

Fig. 15. Biosorption efficiency of CPW towards MB and MG removal upto five successive regeneration cycles.

removal efficiency was observed upto the five cycles. The results of the regeneration of both the dyes MB and MG was maintained more than 80% removal efficiency in all the recycles carried out. The study of desorption and regeneration studies revealed that the CPW possessed potential recycle performance.

4. Conclusions

The locally available and cheap biomass of *Carica papaya* wood (CPW) used as the biosorbent for removal the cationic dyes MB and MG from the aqueous solutions without any laborious pre treatment. The examination of the CPW characterization revealed that the rough surface, cavities, large pores and functional groups distribution on the biosorbent had made the effective dyes sequestrations. The obtained results of biosorption parameters showed that the efficiency of MB, MG removal depends on the initial solution pH, CPW dose, contact time, initial dye concentration and temperature. The optimum initial dye solution pH for the removal of both MB and MG was found as 10.0. The biosorption experimental data were analyzed by using Langmuir, Freundlich, Dubinin–Radushkevich, Temkin, Jovanovic, Halsey and Flory–Huggins isotherm models. The biosorption behavior of CPW towards MB and MG removal was best described by the Langmuir isotherm model and the values of coefficient of determination was greater than 0.990. The rate of the biosorption process was inspected using the kinetic models of pseudo-first-order, pseudo-second-order, Elovich and intraparticle diffusion. Biosorption kinetic analysis indicated that pseudo-second-order kinetic model fitted very well for the biosorption of MG, MB onto CPW with the coefficient of determination values of greater than 0.997. The temperature dependent data of thermodynamic study for the different initial dye concentrations showed that the biosorption process of both the dyes was spontaneous and endothermic. The effect of NaCl results implied that the dyes biosorption performance of CPW was consistent even at the higher ionic strength of NaCl. The regeneration experiments demonstrated that the CPW retained the better biosorption capacity towards the removal of MB and MG for all five subsequent cycles examined. A comparison between maximum biosorption capacities of CPW towards dyes removal with other biosorbents are presented in Table 7. CPW showed relatively better biosorption potential for the removal of both MB and MG. The availability and cost effectiveness of Carica papaya wood will provide a cheap source of biosorbent for the sequestration of toxic dyes from industrial effluents.

Acknowledgements

References

[1] A. Ahmad, M. Rafatullah, O. Sulaiman, M.H. Ibrahim, R. Hashim, Scavenging behaviour of meranti sawdust in the removal of methylene blue from aqueous solution, J. Hazard. Mater 170 (2009) 357–365.

[2] M. Ghaedi, S. Hajati, B. Barazesh, F. Karimi, G. Ghezelbash, *Saccharomyces cerevisiae* for the biosorption of basic dyes from binary component systems and the high order derivative spectrophotometric method for simultaneous analysis of Brilliant green and Methylene blue, J. Ind. Eng. Chem. 19 (2013) 227–233.

[3] S.S. Kumar, P. Balasubramanian, G. Swaminathan, Degradation potential of free and immobilized cells of white rot fungus *Phanerochaete chrysosporium* on synthetic dyes, Int. J. Chem. Tech. Res. 5 (2013) 565–571.

[4] E. Daneshvar, A. Vazirzadeh, A. Niazi, M. Sillanpaa, A. Bhatnagar, A comparative study of methylene blue biosorption using different modified brown, red and green macroalgae – effect of pretreatment, Chem. Eng. J. 307 (2017) 435–446.

[5] J. Song, W. Zou, Y. Bian, F. Su, R. Han, Adsorption characteristics of methylene blue by peanut husk in batch and column modes, Desalination 265 (2011) 119–125.

[6] V. Vimonses, S. Lei, B. Jin, C.W.K. Chow, C. Saint, Kinetic study and equilibrium isotherm analysis of Congo Red adsorption by clay materials, Chem. Eng. J. 148 (2009) 354–364.

[7] Z. Liu, F. Zhang, T. Liu, N. Peng, C. Gai, Removal of azo dye by a highly graphitized and heteroatom doped carbon derived from fish waste: Adsorption equilibrium and kinetics, J. Environ. Manage. 182 (2016) 446–454.

[8] S. Baruah, A. Devi, K.G. Bhattacharyya, A. Sarma, Developing a biosorbent from *Aegle Marmelos* leaves for removal of methylene blue from water, Int. J. Environ. Sci. Technol. (2016), http://dx.doi.org/10.1007/s13762-016-1150-9.

[9] H. Singh, G. Chauhan, A.K. Jain, S.K. Sharma, Adsorptive potential of agricultural wastes for removal of dyes from aqueous solutions, J. Environ. Chem. Eng. 5 (2017) 122–135.

[10] M.K. Dahri, M.R.R. Kooh, L.B.L. Lim, Application of *Casuarina equisetifolia* needle for the removal of methylene blue and malachite green dyes from aqueous solution, Alexandria Eng. J. 54 (2015) 1253–1263.

[11] M. Rafatullah, O. Sulaiman, R. Hashim, A. Ahmad, Adsorption of methylene blue on low-cost adsorbents: a review, J. Hazard. Mater. 177 (2010) 70–80.

[12] M.K. Dahri, M.R.R. Kooh, L.B.L. Lim, Water remediation using low cost adsorbent walnut shell for removal of malachite green: Equilibrium, kinetics, thermodynamic and regeneration studies, J. Environ. Chem. Eng. 2 (2014) 1434–1444.

[13] E.K. Guechi, O. Hamdaoui, Sorption of malachite green from aqueous solution by potato peel: Kinetics and equilibrium modeling using non-linear analysis method, Arab. J. Chem. 9 (2016) S416–S424.

[14] F. Deniz, Dye removal by almond shell residues: Studies on biosorption performance and process design, Mater. Sci. Eng. C Mater. Biol. Appl. 33 (2013) 2821–2826.

[15] X.P. Luo, S.Y. Fu, Y.M. Du, J.Z. Guo, B. Li, Adsorption of methylene blue and malachite green from aqueous solution by sulfonic acid group modified MIL-101, Micropor. Mesopor. Mater 237 (2017) 268–274.

[16] A.R. Khataee, F. Vafaei, M. Jannatkhah, Biosorption of three textile dyes from contaminated water by filamentous green algal *Spirogyra* sp.: Kinetic, isotherm and thermodynamic studies, Int. Biodeterior. Biodegrad. 83 (2013) 33–40.

[17] N.E. Messaoudi, M.E. Khomri, A. Dbik, S. Bentahar, A. Lacheraia, B. Bakiz, Biosorption of Congo red in a fixed-bed column from aqueous solution using jujube shell: Experimental and mathematical modeling, J. Environ. Chem. Eng. 4 (2016) 3848–3855.

[18] S. Rangabhashiyam, N. Anu, N. Selvaraju, Sequestration of dye from textile industry wastewater using agricultural waste products as adsorbents, J. Environ. Chem. Eng. 1 (2013) 629–641.

[19] M.E. Haddad, A. Regti, R. Slimani, S. Lazar, Assessment of the biosorption kinetic and thermodynamic for the removal of safranin dye from aqueous solutions using calcined mussel shells, J. Ind. Eng. Chem. 20 (2014) 717–724.

[20] A. Abdolali, W.S. Guo, H.H. Ngo, S.S. Chen, N.C. Nguyen, K.L. Tung, Typical lignocellulosic wastes and by-products for biosorption process in water and wastewater treatment: a critical review, Bioresour. Technol. 160 (2014) 57–66.

[21] S. Rangabhashiyam, E. Suganya, N. Selvaraju, LityAlen Varghese, Significance of exploiting non-living biomaterials for the biosorption of wastewater pollutants, World. J. Microbiol. Biotechnol. 30 (2014) 1669–1689.

[22] K. Vijayaraghavan, S. Rangabhashiyam, T. Ashokkumar, Jesu Arockiaraj, Assessment of samarium biosorption from aqueous solution by brown macroalga *Turbinaria conoides*, J. Taiwan Inst. Chem. Eng. 74 (2017) 113–120.

[23] M.A. Waha, S. Jellali, N. Jedidi, Ammonium biosorption onto sawdust: FTIR analysis, kinetics and adsorption isotherms modeling, Bioresour. Technol. 101 (2010) 5070–5075.

[24] G.O.E. Sayed, Removal of methylene blue and crystal violet from aqueous solutions by palm kernel fiber, Desalination 272 (2011) 225–232.

[25] M. Dogan, H. Abak, M. Alkan, Adsorption of methylene blue onto hazelnut shell: Kinetics, mechanism and activation parameters, J. Hazard. Mater. 164 (2009) 172–181.

[26] U.J. Etim, S.A. Umoren, U.M. Eduok, Coconut coir dust as a low cost adsorbent for the removal of cationic dye from aqueous solution, J. Saudi. Chem. Soc. 9 (2012) 12–18.

[27] X. Han, W. Wang, X. Ma, Adsorption characteristics of methylene blue onto low cost biomass material lotus leaf, Chem. Eng. J. 171 (2011) 1–8.

[28] N. Boudechiche, H. Mokaddem, Z. Sadaoui, M. Trari, Biosorption of cationic dye from aqueous solutions onto lignocellulosic biomass (*Luffa cylindrica*): characterization, equilibrium, kinetic and thermodynamic studies, J. Ind. Eng. Chem. 7 (2016) 167–180.

[29] A.B. Albadarin, C. Mangwandi, Mechanisms of Alizarin Red S and Methylene blue biosorption onto olive stone by-product: isotherm study in single and binary systems, J. Environ. Manage. 164 (2015) 86–93.

[30] B. Sadhukhan, N.K. Mondal, S. Chattoraj, Optimisation using central composite design (CCD) and the desirability function for sorption of methylene blue from aqueous solution onto *Lemna major*, Karbala Int. J. Modern Sci. 2 (2016) 145–155.

[31] B. Sadhukhan, N.K. Mondal, S. Chattoraj, Biosorptive removal of cationic dye from aqueous system: a response surface methodological approach, Clean Tech. Environ. Policy 16 (2014) 1015–1025.

[32] M.S.U. Rehman, I. Kim, J.I. Han, Adsorption of methylene blue dye from aqueous solution by sugar extracted spent rice biomass, Carbohydr. Polym. 90 (2012) 1314–1322.

[33] M.T. Uddin, M.A. Islam, S. Mahmud, M. Rukanuzzaman, Adsorptive removal of methylene blue by tea waste, J. Hazard. Mater. 164 (2009) 53–60.

[34] A.E. Ofomaja, Kinetic study and sorption mechanism of methylene blue and methyl violet onto mansonia (*Mansonia altissima*) wood sawdust, Chem. Eng. J. 143 (2008) 85–95.

[35] F.A. Pavan, E.C. Lima, S.L.P. Dias, A.C. Mazzocato, Methylene blue biosorption

from aqueous solutions by yellow passion fruit waste, J. Hazard. Mater. 150 (2008) 703–712.

[36] M. Rahimdokht, E. Pajootan, M. Arami, Central composite methodology for methylene blue removal by *Elaeagnus angustifolia* as a novel biosorbent, J. Environ. Chem. Eng. 4 (2016) 1407–1416.

[37] T. Santhi, S. Manonmani, T. Smitha, Removal of malachite green from aqueous solution by activated carbon prepared from the epicarp of *Ricinus communis* by adsorption, J. Hazard. Mater. 179 (2010) 178–186.

[38] M.A Ahmad, R. Alrozi, Removal of malachite green dye from aqueous solution using rambutan peel-based activated carbon: Equilibrium, kinetic and thermodynamic studies, Chem. Eng. J. 171 (2011) 510–516.

[39] A.W. Krowiak, Analysis of influence of process conditions on kinetics of malachite green biosorption onto beech sawdust, Chem. Eng. J. 171 (2011) 976–985.

[40] X.S. Wang, Invasive freshwater macrophyte alligator weed: novel adsorbent for removal of malachite green from aqueous solution, Water Air Soil Pollut. 206 (2010) 215–223.

[41] M.P. Premkumar, V.V Kumar, P.S. Kumar, P. Baskaralingam, V. Sathyaselvabala, T. Vidhyadevi, S. Sivanesan, Kinetic and equilibrium studies on the biosorption of textile dyes onto *Plantago ovata* seeds, Korean J. Chem. Eng. 30 (2013) 1248–1256.

[42] S. Nethaji, A. Sivasamy, G. Thennarasu, S. Saravanan, Adsorption of Malachite Green dye onto activated carbon derived from *Borassus aethiopum* flower biomass, J. Hazard. Mater. 181 (2010) 271–280.

[43] V.K Garg, R. Kumar, R. Gupta, Removal of malachite green dye from aqueous solution by adsorption using agro-industry waste: a case study of *Prosopis cineraria*, Dyes Pigm. 62 (2004) 1–10.

[44] A.A. Jalil, S. Triwahyono, M.R. Yaakob, Z.Z.A. Azmi, N. Sapawe, N.H.N. Kamarudin, H.D. Setiabudi, N.F. Jaafar, S.M. Sidik, S.H. Adam, B.H. Hameed, Utilization of bivalve shell-treated *Zea mays* L. (maize) husk leaf as a low-cost biosorbent for enhanced adsorption of malachite green, Bioresour. Technol. 120 (2012) 218–224.

[45] B. Mi-Hwa, I. Christianah Olakitan, O. Se-Jin, K. Dong-Su, Removal of malachite green from aqueous solution using degreased coffee bean, J. Hazard. Mater. 176 (2010) 820–828.

[46] Z.M. Magriotis, M.Z. Carvalho, P.F. Sales, F.C. Alves, R.F. Resende, A.A. Saczk, Castor bean (*Ricinus communis* L.) presscake from biodiesel production: An efficient low cost adsorbent for removal of textile dyes, J. Environ. Chem. Eng. 2 (2014) 1731–1740.

[47] T. Vij, Y. Prashar, A review on medicinal properties of *Carica papaya* Linn. Asian Pac. J. Trop. Dis. 5 (2015) 1–6.

[48] S. Basha, Z.V.P. Murthy, B. Jha, Sorption of Hg(II) onto Carica papaya: experimental studies and design of batch sorber, Chem. Eng. J. 147 (2009) 226–234.

[49] B.C. Oei, S. Ibrahim, S. Wang, H.M. Ang, Surfactant modified barley straw for removal of acid and reactive dyes from aqueous solution, Bioresour. Technol. 100 (2009) 4292–4295.

[50] R.L. Zorica, D.S. Mirjana, B.M. Smilja, V.M. Jelena, L.M. Marija, S.K.R. Tatjana, L.J.K. Mirjana, Effects of different mechanical treatments on structural changes of lignocellulosic waste biomass and subsequent Cu(II) removal kinetics, Arab. J. Chem. (2016), http://dx.doi.org/10.1016/j.arabjc.2016.04.005.

[51] S. Rangabhashiyam, N. Selvaraju, Adsorptive remediation of hexavalent chromium from synthetic wastewater by a natural and ZnCl$_2$ activated *Sterculia guttata* shell, J. Mol. Liq. 207 (2015) 39–49.

[52] T. Akar, B. Anilan, A. Gorgulu, S.T. Akar, Assessment of cationic dye biosorption characteristics of untreated and non-conventional biomass: *Pyracantha coccinea* berries, J. Hazard. Mater. 168 (2009) 1302–1309.

[53] R. Han, L. Zhang, C. Song, M. Zhang, H. Zhu, L. Zhang, Characterization of modified wheat straw, kinetic and equilibrium study about copper ion and methylene blue adsorption in batch mode, Carbohydr. Polym. 79 (2010) 1140–1149.

[54] M.C. Somasekhara Reddy, L. Sivaramakrishna, A. Varada Reddy, The use of an agricultural waste material, Jujuba seeds for the removal of anionic dye (Congo red) from aqueous medium, J. Hazard. Mater. 203–204 (2012) 118–127.

[55] N.F. Cardoso, E.C. Lima, B. Royer, M.V. Bach, G.L. Dotto, L.A.A. Pinto, T. Calvete, Comparison of Spirulina platensis microalgae and commercial activated carbon as adsorbents for the removal of reactive Red 120 dye from aqueous effluents, J. Hazard. Mater. 241–242 (2012) 146–153.

[56] P.S. Kumar, S. Ramalingam, C. Senthamarai, M. Niranjanaa, P. Vijayalakshmi, S. Sivanesan, Adsorption of dye from aqueous solution by cashew nut shell: studies on equilibrium isotherm, kinetics and thermodynamics of interactions, Desalination 261 (2010) 52–60.

[57] N. Gupta, A.K. Kushwaha, M.C. Chattopadhyaya, Adsorption studies of cationic dyes onto Ashoka (*Saraca asoca*) leaf powder, J. Taiwan Inst. Chem. Eng. 43 (2012) 604–613.

[58] S.A. Wagner, A. Elie, C.L. Eder, R. Betina, E.S. Felipe, L. Jeronimo, N.A. Claudio, Application of *Mangifera indica* (mango) seeds as a biosorbent for removal of Victazol Orange 3R dye from aqueous solution and study of the biosorption mechanism, Chem. Eng. J. 209 (2012) 577–588.

[59] Z. Sunxiang, Z. Tongshui, Biosorption of methylene blue from wastewater by an extraction residue of *Salvia miltiorrhiza Bge*, Bioresour. Technol. 219 (2016) 330–337.

[60] F. Doulati Ardejani, Kh. Badii, N. Yousefi Limaee, S.Z. Shafaei, A.R. Mirhabibi, Adsorption of Direct Red 80 dye from aqueous solution onto almond shells: Effect of pH, initial concentration and shell type, J. Hazard. Mater. 151 (2008) 730–737.

[61] M.A. Tahir, H.N. Bhatti, M. Iqbal, Solar Red and Brittle Blue direct dyes adsorption onto *Eucalyptus angophoroides* bark: Equilibrium, kinetics and thermodynamic studies, J. Environ. Chem. Eng. 4 (2016) 2431–2439.

[62] H. Warda, F. Umar, A. Muhammad, A. Makshoof, A.K. Misbahul, Potential

[63] M.M. Seyed, K.N. Soheil, Mohammad P, A. Nima, V. Leila, M. Gordon, Methylene blue adsorption via maize silk powder: Kinetic, equilibrium, thermodynamic studies and residual error analysis, Process Saf. Environ. Prot. 106 (2017) 191–202.

[64] Y. Tang, Y. Zeng, T. Hu, Q. Zhou, Y. Peng, Preparation of lignin sulfonate-based mesoporous materials for adsorbing malachite green from aqueous solution, J. Environ. Chem. Eng. 4 (2016) 2900–2910.

[65] M.T. Yagub, T.K. Sen, H.M. Ang, Equilibrium, kinetics, and thermodynamics of methylene blue adsorption by pine tree leaves, Water Air Soil Pollut 223 (2012) 5267.

[66] O. Fumihiko, I. Daisuke, K. Naohito, Cationic dye removal from aqueous solution by waste biomass produced from calcination treatment of rice bran, J. Environ. Chem. Eng. 3 (2015) 1476–1485.

[67] M.C. Ncibi, Applicability of some statistical tools to predict optimum adsorption isotherm after linear and non-linear regression analysis, J. Hazard. Mater. 153 (2008) 207–212.

[68] S. Rangabhashiyam, N. Anu, M.S. Giri Nandagopal, N. Selvaraju, Relevance of isotherm models in biosorption of pollutants by agricultural byproducts, J. Environ. Chem. Eng. 2 (2014) 398–414.

[69] I. Langmuir, The adsorption of gases on plane surfaces of glass, mica and platinum, J. Am. Chem. Soc. 40 (1918) 1361–1403.

[70] K.R. Hall, L.C. Eagleton, A. Acrivos, T. Vermeulen, Pore and solid diffusion kinetics in fixed bed adsorption under constant pattern conditions, Ind. Eng. Chem. Fund. 5 (1966) 212–219.

[71] H.M.F. Freundlich, Uber die adsorption in losungen, Z. Phys. Chem. 57A (1906) 385–470.

[72] M.M. Dubinin, E.D. Zaverina, L.V. Radushkevich, Sorption and structure of active carbons. I. Adsorption of organic vapors, Zh. Fiz. Khim. 21 (1947) 1351–1362.

[73] M.J. Tempkin, V. Pyzhev, Kinetics of ammonia synthesis on promoted iron catalysts, A. Physiochim. URSS 12 (1940) 217–222.

[74] D.S. Jovanovic, Physical adsorption of gases I: isotherms formonolayer and multilayer adsorption, Colloid Polym. Sci. 235 (1969) 1203–1214.

[75] G. Halsey, Physical adsorption on nonuniform surfaces, J. Chem. Phys. 16 (1948) 931–937.

[76] M. Horsfall, A.I. Spiff, Equilibrium sorption study of Al^{3+}, Co^{2+} and Ag^{2+} in aqueous solutions by fluted pumpkin (*Telfairia occidentalis* HOOK) waste biomass, Acta Chim. Slov. 52 (2005) 174–181.

[77] T. Akar, S. Celik, S.T. Akar, Biosorption performance of surface modified biomass obtained from *Pyracantha coccinea* for the decolorization of dye contaminated solutions, Chem. Eng. J. 160 (2010) 466–472.

[78] S. Liang, X. Guo, N. Feng, Q. Tian, Isotherms, kinetics and thermodynamic studies of adsorption of Cu^{2+} from aqueous solutions by Mg^{2+}/K$^+$ type orange peel adsorbents, J. Hazard. Mater. 174 (2010) 756–762.

[79] S. Lagergren, About the theory of so-called adsorption of soluble substances, K. Svenska Vetenskapsakad. Handl. 24 (1898) 1–39.

[80] Y.S. Ho, G. McKay, Pseudo-second order model for sorption processes, Process Biochem 34 (1999) 451–465.

[81] F.C. Wu, R.L. Tseng, R.S. Juang, Characteristics of Elovich equation used for the analysis of adsorption kinetics in dye-chitosan systems, Chem. Eng. J. 150 (2009) 366–373.

[82] D. Fatih, D.S. Saadet, Equilibrium, kinetic and thermodynamic studies of Acid Orange 52 dye biosorption by *Paulownia tomentosa* Steud. leaf powder as a low-cost natural biosorbent, Bioresour. Technol. 101 (2010) 5137–5143.

[83] W.J. Weber, J.C. Morris, Advances inwater pollution research: removal of biologically resistant pollutants from waste waters by adsorption, Proceedings of International Conference on Water Pollution Symposium, 2 Pergamon Press, Oxford, 1962, pp. 231–266.

[84] P. Geetha, M.S. Latha, Mathew Koshy, Biosorption of malachite green dye from aqueous solution by calcium alginate nanoparticles: Equilibrium study, J. Mol. Liq. 212 (2015) 723–730.

[85] S. Rangabhashiyam, N. Selvaraju, Efficacy of unmodified and chemically modified *Swietenia mahagoni* shells for the removal of hexavalent chromium from simulated wastewater, J. Mol. Liq. 209 (2015) 487–497.

[86] D. Mitrogiannis, G. Markou, A. Celekli, H. Bozkurt, Biosorption of methylene blue onto *Arthrospira platensis* biomass: Kinetic, equilibrium and thermodynamic studies, J. Environ. Chem. Eng. 3 (2015) 670–680.

[87] G. Jian-Zhong, L. Bing, L. Li, L. Kangle, Removal of methylene blue from aqueous solutions by chemically modified bamboo, Chemosphere 111 (2014) 225–231.

[88] H. Runping, W. Yuanfeng, H. Pan, S. Jie, Y. Jian, L. Yongsen, Removal of methylene blue from aqueous solution by chaff in batch mode, J. Hazard. Mater. 137 (2006) 550–557.

[89] M.C. Ncibi, B. Mahjoub, M. Seffen, Kinetic and equilibrium studies of methylene blue biosorption by *Posidonia oceanica* (L.) fibres, J. Hazard. Mater. 139 (2007) 280–285.

[90] P.S. Kumara, R.V. Abhinaya, K.G. Lashmi, V. Arthi, R. Pavithra, V. Sathyaselvabala, S.D. Kirupha, S. Sivanesan, Adsorption of methylene blue dye from aqueous solution by agricultural waste: equilibrium, thermodynamics, kinetics, mechanism and process design, Colloid J. 73 (2011) 647–657.

[91] U.J. Etim, S.A. Umoren, U.M. Eduok, Coconut coir dust as a low cost adsorbent for the removal of cationic dye from aqueous solution, J. Saudi Chem. Soc. 9 (2012) 12–18.

[92] K.G. Bhattacharyya, A. Sharma, Kinetics and thermodynamics of methylene blue adsorption on neem (*Azadirachta indica*) leaf powder, Dyes Pigm. 65 (2005) 51–59.

[93] M. Kumar, R. Tamilarasan, Modeling studies for the removal of methylene blue

from aqueous solution using *Acacia fumosa* seed shell activated carbon, J. Environ. Chem. Eng. 1 (2013) 1108–1116.

[94] T. Sarat Chandra, S.N. Mudliar, S. Vidyashankar, S. Mukherji, R. Sarada, K. Krishnamurthi, V.S. Chauhan, Defatted algal biomass as a non-conventional low-cost adsorbent: Surface characterization and methylene blue adsorption characteristics, Bioresour. Technol. 184 (2015) 395–404.

[95] S.D. Khattri, M.K. Singh, Colour removal from dye wastewater using sugar cane dust as an adsorbent, Adsorpt. Sci. Technol. 17 (1999) 269–282.

[96] P. Saha, S. Chowdhury, S. Gupta, I. Kumar, R. Kumar, Assessment on the removal of malachite green using tamarind fruit shell as biosorbent, Clean 38 (2010) 437–445.

[97] K.V. Kumar, S. Sivanesan, Isotherms for Malachite Green onto rubber wood (*Hevea brasiliensis*) sawdust: Comparison of linear and non-linear methods, Dyes Pigm. 72

(2007) 124–129.

[98] B. Zehra, S. Yoldas, C. Levent, Removal of malachite green by using an invasive marine alga *Caulerpa racemosa* var. *cylindracea*, J. Hazard. Mater. 161 (2009) 1454–1460.

[99] T. Santhi, S. Manonmani, V.S. Vasantha, Y.T. Chang, A new alternative adsorbent for the removal of cationic dyes from aqueous solution, Arab. J. Chem. 9 (2016) S466–S474.

[100] N. Gupta, A.K. Kushwaha, M.C. Chattopadhyaya, Kinetics and thermodynamics of malachite green adsorption on banana pseudo-stem fibers, J. Chem. Pharm. Res. 3 (2011) 284–296.

[101] A.K. Kushwaha, N. Gupta, M.C. Chattopadhyaya, Removal of cationic methylene blue and malachite green dyes from aqueous solution by waste materials of *Daucus carota*, J. Saudi Chem. Soc. 18 (2014) 200–207.